forests

MDPI

Article

Temperature Sensitivity of CO_2 and CH_4 Fluxes from Coarse Woody Debris in Northern Boreal Forests

Liudmila Mukhortova [1,*], Natalia Pashenova [1], Maria Meteleva [1], Leonid Krivobokov [1] and Georg Guggenberger [1,2]

[1] Sukachev Institute of Forest SB RAS, Federal Research Center "Krasnoyarsk Science Center SB RAS", Akademgorodok 50-28, 660036 Krasnoyarsk, Russia; pasnat@ksc.krasn.ru (N.P.); innerself@ksc.krasn.ru (M.M.); leo_kr@mail.ru (L.K.); guggenberger@ifbk.uni-hannover.de (G.G.)
[2] Institute of Soil Science, Leibniz Universität Hannover, Herrenhäuser Str. 2, 30419 Hannover, Germany
* Correspondence: l.mukhortova@gmail.com

Abstract: Carbon dioxide (CO_2) and methane (CH_4) are recognized as the main greenhouse gases causing climate warming. In forest ecosystems, the death of trees leads to the formation of coarse woody debris (CWD) that is one of the sources of greenhouse gas emissions due to wood decomposition. We quantified the CO_2 and CH_4 fluxes from CWD of larch (*Larix gmelinii* (Rupr.)) and birch (*Betula tortuosa* Ledeb.) collected in the northern boreal forests of Central Siberia. The CWD samples were incubated at +5, +15 and +25 °C. The CO_2 and CH_4 fluxes showed strong correlations with temperature, moisture, decomposition stage and the type of wood's rot. The temperature coefficient Q_{10} indicated higher temperature sensitivity of CO_2 flux within the temperature interval from +5 to +15 °C than from +15 to +25 °C. Methane flux had higher temperature sensitivity within the interval from +15 to +25 °C. It was found that, in boreal forests, CWD of early decay stage can serve as a source of methane to the atmosphere when air temperatures increased above +15 °C. Strong positive correlation between CH_4 production and CO_2 emission indicated a biological source and supported findings on aerobic origin of the main process contributing to the CH_4 flux from decomposing CWD.

Keywords: boreal forests; coarse woody debris; carbon dioxide and methane emission; methane production and consumption; temperature response

Citation: Mukhortova, L.; Pashenova, N.; Meteleva, M.; Krivobokov, L.; Guggenberger, G. Temperature Sensitivity of CO_2 and CH_4 Fluxes from Coarse Woody Debris in Northern Boreal Forests. *Forests* **2021**, *12*, 624. https://doi.org/10.3390/f12050624

Academic Editor: Matthias Peichl

Received: 26 February 2021
Accepted: 11 May 2021
Published: 14 May 2021

1. Introduction

The increase in atmospheric greenhouse gas concentrations is one of the main reasons of the contemporary climate change [1], and carbon dioxide (CO_2) and methane (CH_4) play the most important role in acceleration of global warming. A significant amount of atmospheric carbon is sequestered in forest ecosystems: in the tree phytomass, dead plant residues and soil organic matter. According to the last estimates, annual carbon accumulation in Russian forests is 250 Mt, and more than 30,000 Mt of carbon is accumulated as wood biomass on the Russian territory [2]. During the growth and development of tree stands, the death of trees is leading to the formation of coarse woody debris (CWD). This is one of the least understood components of forest ecosystems [3]. Due to the high possibility of global carbon balance underestimation, the interest to CWD increased during the last decades [4].

Dead wood in the native boreal forests usually does not contribute much to greenhouse gases in the atmosphere due to the low rate of CWD decomposition [3]. However, in disturbed ecosystems (e.g., post-fire ecosystems, after the windfall, post-logging ecosystems and in the forests destroyed by pests), the amount of dead wood can increase significantly, thus turning into an important source of carbon dioxide emission [3,5–8]. Besides, the greenhouse gas emission from CWD can play a crucial role during spring and autumn, when the photosynthetic ability of plants is decreased [9]. This could be one of the reasons of observed seasonal fluctuations of atmospheric carbon in the Northern Hemisphere [9,10].

The field of our interest covers the permafrost region of Siberia. This region is of vital importance for the planetary processes since the strongest warming is observed in the high latitudes of the Earth [11]. More than 35% of the forest lands on permafrost in Russia are larch forests [12]. In Siberia, larch forms monodominant stands, which cover 84% and 93% of forested area in the northern boreal subzone and in the forest-tundra zone, respectively [13–15]. Birch forests are also widespread in the northern boreal subzone, especially in Central Siberia [16,17]. These northern forests are recognized as the most sensitive to the climate change [11,18] since they grow at temperatures which are currently limiting both biomass productivity and decomposition rate.

In the mature and old-growth larch forests of this region, CWD stock vary from 2 to 8 t ha^{-1} [19], that is, 17–21% of total stand biomass in these ecosystems [20] or about 4% of ecosystem total carbon stock [21]. In the region under study, fire is the major disturbing factor, the average interval of fire events is about 80 years [22]. In postfire ecosystems, stock of CWD can increase by 60–100%, reaching 200% of tree stand biomass 10 years after the fire [19,20]. Carbon stock in this dead wood can comprise 6.5–8.0 tC ha^{-1} in these postfire ecosystems [19].

A very significant increase of the surface air temperatures is already observed in the high latitudes [23], and the key question now is how strong different components of the northern forest ecosystems will react on this temperature rising? On the one hand, climate warming can lead to the increase of CWD stock due to the increment of forest fires and drought frequency in this region [24–26]. At the same time, higher temperatures can increase the rate of CWD decomposition [27]. Both of these developments might mean an enhancement of the flux of greenhouse gases from the pool of CWD from these forests [28].

One of the most common measure of temperature sensitivity mentioned in the scientific literature is the temperature coefficient Q_{10} that shows how much the rate of the process is altered with temperature increase by 10 °C [29]. However, Q10 is a relative measure so that some other approaches should be involved to estimate the real values of the changed rate [30].

In our study, we decided to focus on CO_2 as well as on CH_4 fluxes, since both carbon forms are released from decomposing wood [31–36]. Carbon dioxide is a product of aerobic decomposer respiration. Methane production (methanogenesis) is mainly an anaerobic respiration [37]. Methanogens are found in all types of anaerobic environments. In addition, recent studies have shown biological and non-microbial methane formation under oxygenated conditions [37–39]. Despite the fact that methane production is possible in a wide range of conditions, not all produced CH_4 will be emitted to the atmosphere. Microbial aerobic and anaerobic CH_4 oxidation (CH_4 consumption) often takes place simultaneously, thereby counteracting the CH_4 production, and reducing the net CH_4 flux [37]. Methane-oxidizing microorganisms consume methane and metabolize it as a source of both carbon and reductant to drive cellular processes [40].

Recently, the measurement of the ratio of stable carbon isotopes have been widely applied to investigate sources and sinks of atmospheric CH_4 [41,42]. The natural abundance of stable carbon isotopes ^{12}C and ^{13}C comprise 98.89% and 1.11%, respectively, of the total carbon on Earth [43]. Measurements of these isotopes are expressed as the ratios to the more common ^{12}C in a sample ($^{13}C/^{12}C$) and reported in the $\delta^{13}C$ notation relative to the Vienna Pee Dee Belemnite (VPDB) standard in per mil (‰) [44]. Physiochemical and biological processes create distinctive carbon isotopic signatures in biogenic material that allow tracing its origin and identifying processes in the nature [45]. Mean carbon isotopic composition of atmospheric methane ($\delta^{13}C$-CH_4) is equal to −47‰ [46]. Microbially produced CO_2 and CH_4 are depleted in ^{13}C in comparison with gases produced by chemical, photochemical or thermal decomposition of organic matter, because metabolic processes preferably use the lighter carbon isotope over the heavier isotope [47–50]. Molecules with the heavier isotope form stronger bonds and have higher activation energies, which makes them more difficult for utilization compared with molecules with lighter isotopes [45]. As a result, biogenic methane have $\delta^{13}C$ equal to -60 ± 5‰, whereas biomass burning, coal mining and nat-

ural gas produce methane with $\delta^{13}C$ varying from -24 ± 3 to -43 ± 7‰ [41]. Microbial oxidation of CH_4, both aerobic and anaerobic, is also associated with fractionation for C isotopes that leads to an enrichment of the residual CH_4 with the heavier isotope [51–53] and a depletion of ^{13}C in the CO_2 pool [54].

Different field and laboratory incubation experiments have been performed, wherein the effects of temperature, moisture and decomposition stage on carbon loss from coarse woody debris were studied, such as the study on boreal black spruce in Manitoba [55], on Sitka spruce in Ireland [56], on Oriental oak and red pine in Korea [57,58], on CWD in Amazon tropical forests [59], and in temperate forests of China and Northern America [60,61]. Each of these studies only estimated the CO_2 flux from decomposing CWD and only one study focused on CH_4 emission from CWD decomposing by saprotrophic fungi [39]. However, to our knowledge, none of these studies have measured CO_2 and CH_4 emissions simultaneously, and the temperature sensitivity of CH_4 flux from CWD was not studied before.

In this study, we aimed to estimate possible changes in greenhouse gas emissions from CWD decomposition under the climate changes. The temperature sensitivity of CO_2 and CH_4 fluxes from decomposing dead wood of larch (*Larix gmelinii* (Rupr.) Rupr) and birch (*Betula tortuosa* Ledeb.), collected in the northern boreal forests of Central Siberia was studied in the laboratory incubation experiments. We quantified also the rates of methane production and methane oxidation in the decomposing wood through assessing the ratio of stable carbon isotopes.

2. Materials and Methods

The area of the study is Central Evenkia (64° N, 100° E) near the Tura settlement. The territory is hilly with gentle slopes within 120–600 m above the sea level, with pronounced erosive formation of valleys. The whole territory is underlain by continuous permafrost, and soils are Cryosols [62].

The climate is cold (continental) without a dry season according to Köppen-Geiger climate classification [63]. The mean annual temperature is −8.9 °C. The annual amplitude of temperature is 52 °C, and the growing degree-days above 10 °C is 1000 °C, while the frost-free period amounts to 70–80 days. Mean annual precipitation is 369 mm. Seasonal distribution of precipitation is approximately even. Snow cover thickness varies within 50–60 cm. The climate differs with the altitude due to the air mass inversions between the foot and summit of mountains [62].

In the studied area, larch (*Larix gmelinii*) and birch (*Betula tortuosa*) stands are predominant. Cowberry (*Vaccinium vitis-idaea* L.), bog bilberry (*Vaccinium uliginosum* L.), marsh tea (*Ledum palustre* L.) and typical boreal mosses (*Pleurozium schreberi* (Brid.) Mitt., *Hylocomium splendens* (Hedw.) Bruch et al., *Aulacomnium palustre* (Hedw.) Schwagr.) are widespread under the tree canopy. In general, birch forests in Evenkia occupy a small area, about 5%, of the overall territory [13]. However, in Central Evenkia, in the Northern boreal subzone, near the Tura settlement, birch forests (*Betula tortuosa*) are widespread, especially on the elevated flat mountain plateau and occupy about 30–40% of the territory [17].

The forest floor in studied ecosystems is covered by laying logs of different stage of decomposition. Decay class of logs was defined in the field according to the system of [64], and three decay classes of CWD were defined based on visual and physical properties. The principle of division was based on wood density and the presence of bark and branches, as follows:

- DC I: Wood has not lost its solidity; log has bark; small to medium branches are present;
- DC II: Wood has lost some of its solidity; bark easily flakes from wood, but bark and larger branches are present on the log;
- DC III: Wood has lost its initial solidity; some bark and large branches can remain on the log.

Discs of larch and birch laying logs were collected each from the same area. Samples were taken at least from three logs of the same decay class for larch and birch. In total

discs of 26 logs were sampled. Diameters of the sampled logs varied from 5.7 to 14.8 cm, representing the prevalent tree diameter within the territory of the study.

For larch logs at DC III, it was possible to identify the type of rot associated with the activity of ligninolytic or cellulolytic basidial fungi (i.e., white rot or brown rot, respectively). The type of rot was determined in the field by visual signs. Thus, for larch at DC III, we measured CO_2 and CH_4 emission for wood decomposed by white and brown rot fungi separately.

Experimental Design

The discs of larch and birch logs at different stages of decomposition were placed in the separate gas-tight plastic boxes of 1500 mL volume. Boxes were hermetically sealed. Immediately after placing the samples in the box and closing, we measured initial concentrations of CO_2 and CH_4 and the stable carbon isotope ratios ($\delta^{13}C$) in these gases in the box headspace using Picarro G2201-i cavity ring-down spectrometer (Picarro, Inc., Santa Clara, USA). We incubated the samples at three different temperatures. At the beginning of the experiment, samples were incubated at +5 °C. The following measurements of CO_2 and CH_4 concentrations were made after 3 h, 24 h, 3 and 6 days. After that, boxes with CWD samples were opened and aerated. The same procedure was afterwards repeated also for other temperature levels (+15 and +25 °C). Before each series of measurements boxes with CWD samples were allowed to equilibrate under specific temperature of the series for 24 h.

At the beginning of each measurement series, the boxes were weighted to trace water loss after aeration. At each measurement, weight loss did not exceed 0.5 g that was less than 5% of sample water content. Woody discs were weighted before experiment and after termination of the experiment they were oven dried at 80 °C until constant weight. Water content (%) was calculated as the ratio of the mass lost (difference between initial and dried weight), attributed to water initially present in the sample, to total mass of the fully dried wood:

$$W = (M_1 - M_2)/M_2 \times 100, \quad (1)$$

where W is the water content in the sample (%), M_1 is the initial weight of the CWD sample (g), and M_2 is the dry weight of the CWD sample (g).

Bulk density of wood was measured for sectors of the woody disc by water displacement method [65]. Carbon and nitrogen contents and the stable carbon isotope ratios in the wood ($\delta^{13}C_{wood}$) were measured using an elemental analyzer (Vario Isotope Cube, Elementar Analysis Systems GmbH, Hanau, Germany) coupled with IRMS (IsoPrime100, Elementar Analysis Systems GmbH, Hanau, Germany). Stable carbon isotope ratios were expressed using the conventional δ notation as ‰ deviations from the Vienna Pee Dee belemnite (VPDB) standard [44,66]:

$$\delta^{13}C = ((R_{sample}/R_{standard}) - 1) \times 1000, \quad (2)$$

where $R = [^{13}C]/[^{12}C]$ for sample and standard, respectively.

The rate of the CO_2 and CH_4 emission ($S_{CO2/CH4}$) was calculated based on the change in concentration of these gases in the box headspace after 24 h of incubation at different temperatures using the following equation:

$$S_{CO2/CH4} = \Delta CO_2(CH_4)/\Delta t \times (V_{air} \times M_{CO2(CH4)})/22.41 \times 273.15/T_{air} \times 1/W_{CWD} \quad (3)$$

where S is CO_2 or CH_4 flux (μg CO_2 g^{-1} h^{-1}), $\Delta CO_2(CH_4)/\Delta t$ is the CO_2 or CH_4 concentration increment (ppm) per time unit (h), V_{air} is the air volume (liter) in the chamber calculated as $V_{air} = V_{chamb} - V_{sample}$ (V_{chamb} is the volume of the chamber, V_{sample} is the volume of CWD sample), $M_{CO2(CH4)}$ is the molar mass of CO_2 (44 g mol^{-1}) or CH_4 (16 g mol^{-1}), T_{air} is the air temperature (K), 22.41 is the molar volume (L mol^{-1}) at the standard temperature (273.15 K) and pressure (1.013 bar), and W_{CWD} is the CWD sample dry weight (g) [58]. Since, as well, CH_4 oxidation as emission could be taking place, the

relative CH_4 increase cannot be used as a direct measure for CH_4 production. For this reason, the isotopic signature of CH_4 was used. It was expected that, during CH_4 consumption, the lighter ^{12}C-CH_4 isotope was preferred. At the same time, CH_4 production was expected to not fractionate.

From here on, we will call the net emission, based on the measured concentration change, the "CH_4 flux". The actual amount of produced CH_4, which we base on studying the isotopic composition of CH_4, we will call the "CH_4 production". The calculated difference between the CH_4 production and the net CH_4 flux, we will call the "CH_4 consumption".

The rate of methane production was calculated based on the assumption that emitted amount of $^{13}CH_4$ reflected the rate of methane production due to isotopic fractionation during methane oxidation. This rate was calculated as following:

1. The amount of evolved $^{13}CH_4$ ($\Delta^{13}CH_4$) was calculated as a difference between concentration of $^{13}CH_4$ measured at the time t and initial $^{13}CH_4$ concentration in the box headspace;
2. Using Equation (2) (the main equation for $\delta^{13}C$), we calculated which amount of $^{12}CH_4$ ($[^{12}CH_4]$) could be produced if supposing that there was no fractionation during methanogenesis and produced methane had $\delta^{13}C$ similar to that in the substrate (wood):

$$R_{CH4} = [^{13}CH_4]/[^{12}CH_4] = R_{standard} \times (\delta^{13}C - CH_{4\_prod}/1000 + 1), \quad (4)$$

where $\delta^{13}C$-CH_{4_prod} is a stable carbon isotopes ratio in produced methane and $\delta^{13}C$-$CH_{4\_prod} = \delta^{13}C_{wood}$.

The amount of $^{12}CH_4$ calculated from Equation (4) is the expected change in $^{12}CH_4$ concentration ($\Delta^{12}CH_4$) in case there would be no methane consumption in decomposing wood.

3. The rate of methane production was calculated for the sum of $\Delta^{12}CH_4$ and $\Delta^{13}CH_4$ using Equation (3).

In these calculations we assumed that there was no fractionation of stable carbon isotopes during methane production in decomposing wood. The stable carbon isotope ratio in methane is reported to vary from −22‰ to as low as −120‰ [45], and the lowest $\delta^{13}C$ values are related to microbially produced methane [67]. However, these values were received mainly for anaerobically produced CH_4. There is no data on the ratio of stable carbon isotopes in methane produced under aerobic conditions. Additionally, we do not know clearly which agents or processes produce methane during wood decomposition. Thus, we supposed that stable carbon isotope ratio in produced methane might be similar to that in the substrate (in the decomposing wood).

The volume of woody samples, which had been incubated for CO_2 and CH_4 flux measurements, varied from 119 to 581 cm^3. As it was shown by Yoon et al. [58], the rate of respiration and methane fluxes from CWD calculated on the weight basis does not depend on the size of wood sample.

To analyze the dependence of CO_2 and CH_4 fluxes on temperature, we calculated relative and absolute measures of temperature sensitivity. We used the Q_{10} coefficient to characterize the relative dependence of CO_2 and CH_4 fluxes on temperature [30]. This coefficient represents the factor by which the rate of biological or chemical processes increases with the temperature increment of 10 °C. This factor was calculated as follows:

$$Q_{10} = (S_2/S_1)^{[10/(T2 - T1)]} \quad (5)$$

where S_1 and S_2 are the rates of CWD respiration or methane fluxes at temperatures T_1 and T_2 [30].

The absolute temperature responses of CO_2 and CH_4 fluxes were calculated as the first derivative of a linear model connecting two rates measured at different temperatures. This model supposes monotonic increase or decrease of the rate within the studied temperature interval. The slope of the line showed how much the rate of studied fluxes had changed with temperature. Calculated temperature response showed changes of the studied fluxes with each degree of temperature.

To avoid confusion we used term "temperature sensitivity" for Q_{10} values and "temperature response" for the absolute changes of CO_2 and CH_4 flux rates with respect to temperature.

Differences in the rate of CO_2 and CH_4 fluxes, and Q_{10} values between species, decomposition classes, and temperature diapasons were analyzed using Mann–Whitney U test. Analysis of variance (ANOVA) and analysis of covariance (ANCOVA) were conducted to assess the overall importance of each influencing factor (tree species, wood density, temperature, and water content).

3. Results

3.1. Bulk Density, Water Content, and Chemical Composition of Studied CWD

Average bulk density of woody samples used in the incubation experiment decreased from DC I to DC III almost twice for larch and almost three times for birch CWD (Table 1). Water content of birch wood samples was three to five times higher than in the samples of larch CWD. Carbon content was similar for samples of all decomposition classes and for both tree species. Only larch wood at the DC III being decomposed by brown rot differed from the other samples by significantly ($p < 0.05$) higher content of carbon. This wood was noticeably depleted in ^{13}C in comparison with wood decomposed by white rot and DC II. Shift of the carbon isotope ratios ($\delta^{13}C$) with decomposition stage was substantially lower for birch wood in comparison with larch wood. The nitrogen content gradually increased from DCI to DC III for wood of both tree species, resulting in lower C to N ratios at the late stage of decomposition. Birch wood at all decomposition classes contained significantly larger amounts of nitrogen than larch wood ($p < 0.05$) (Table 1).

Table 1. The main characteristics of the coarse woody debris samples used in the experiment.

Decomposition Class	Bulk Density, g cm^{-3}	Water Content, %	Carbon		Nitrogen, %	C:N
			%	$\delta^{13}C_{wood}$, ‰		
			Larch			
DC I	0.392 (0.018)	41.8 (11.9)	47.6 (0.14)	−26.4 (1.48)	0.060 (0.008)	819 (108.0)
DC II	0.396 (0.019)	29.4 (10.2)	47.8 (0.25)	−24.8 (0.33)	0.092 (0.008)	564 (66.9)
DC III w	0.204 (0.031)	46.7 (25.5)	47.2 (0.19)	−25.3 (0.30)	0.267 (0.116)	201 (57.6)
DC III b	0.291 (0.014)	99.4 (48.0)	49.5 (0.54)	−26.6 (0.40)	0.235 (0.061)	229 (53.5)
			Birch			
DC I	0.449 (0.015)	117.6 (4.5)	47.5 (0.28)	−26.7 (0.43)	0.157 (0.041)	322 (69.1)
DC II	0.373 (0.020)	163.7 (38.9)	47.4 (0.19)	−27.2 (0.26)	0.109 (0.007)	436 (30.8)
DC III	0.159 (0.014)	449.9 (79.7)	47.2 (0.97)	−27.1 (0.17)	0.348 (0.067)	141 (22.9)

Values are the mean (±SE) of three-seven replicates. Index letters: w—for white rotted wood; b—for brown rotted wood.

3.2. CO_2 Flux from Decomposing CWD Samples

Curve shapes of cumulative carbon dioxide yield during 144 h incubation indicated saturation with time (Figures S1 and S2). The $\delta^{13}C$ ratio in CO_2 decreased during incubation from ambient −12–−13‰ to −23–−33‰. The $\delta^{13}C$-CO2 equal to −23–−33‰ is the result of mixing: the produced CO_2 mixed with CO_2 of the air (with $\delta^{13}C$ = −12–−13‰). In order to shift the ambient isotopic ratio to values that produced CO_2 it must have a lower isotopic signature than in the wood (−24–−26‰). It means that some isotopic fractionation took place during CO_2 production, which is a sign of biological decomposition of wood organic

matter. The calculated rate of CO_2 emission during the first 24 h of incubation showed strong dependence on temperature (Figure 1).

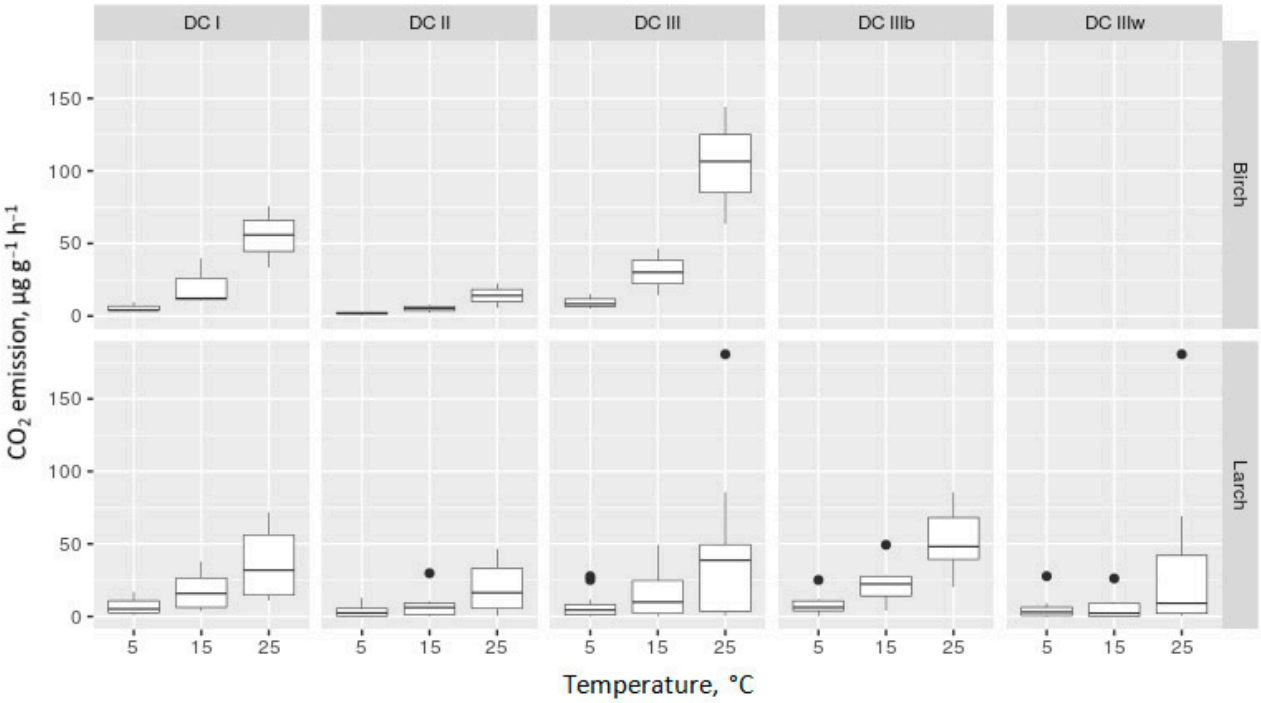

Figure 1. The rate of CO_2 emission during decomposition of larch (Larch) and birch (Birch) wood, shown as box plots (box is an interquartile range (from 25th percentile to 75th percentile), horizontal line is a median value, vertical lines are a range between minimum and maximum values, dots are an outliers): DC I–DC III—decomposition classes I–III; DC IIIw—separately, larch wood of DC III decomposed by white rot fungi; DC IIIb—separately, larch wood of DC III decomposed by brown rot.

At the advanced stage of decomposition (DC III), the CO_2 flux from larch CWD mostly depended on the fungi participating in the decomposition. Decay by brown rot fungi resulted in the release of more than twice a higher amount of CO_2 in comparison with wood decomposed by white rot.

Birch wood produced a higher amount of CO_2 than larch wood during incubation at temperatures +15 and +25 °C. The highest rate of CO_2 emission from birch wood was observed at the decomposition stage DC III.

3.3. Methane Fluxes from Decomposing CWD Samples

Measured flux of CH_4, calculated as methane concentration changes in the headspace of the experimental box during incubation, is the result of two contrary directed processes: methane production and methane consumption. It characterizes the rate of CH_4 flux during decomposition of CWD. In some cases, when during incubation the concentration of CH_4 decreased in the experimental volume, the rate of methane flux was negative indicating evident methane oxidation. However, even if CH_4 increased in the headspace during incubation, CH_4 uptake might still take place, but it was just not dominant.

The calculated rate of CH_4 exchange had no significant dependance on temperature; however, some trend of negative rates of this flux was observed for DC III both for larch and for birch wood (Figure 2a).

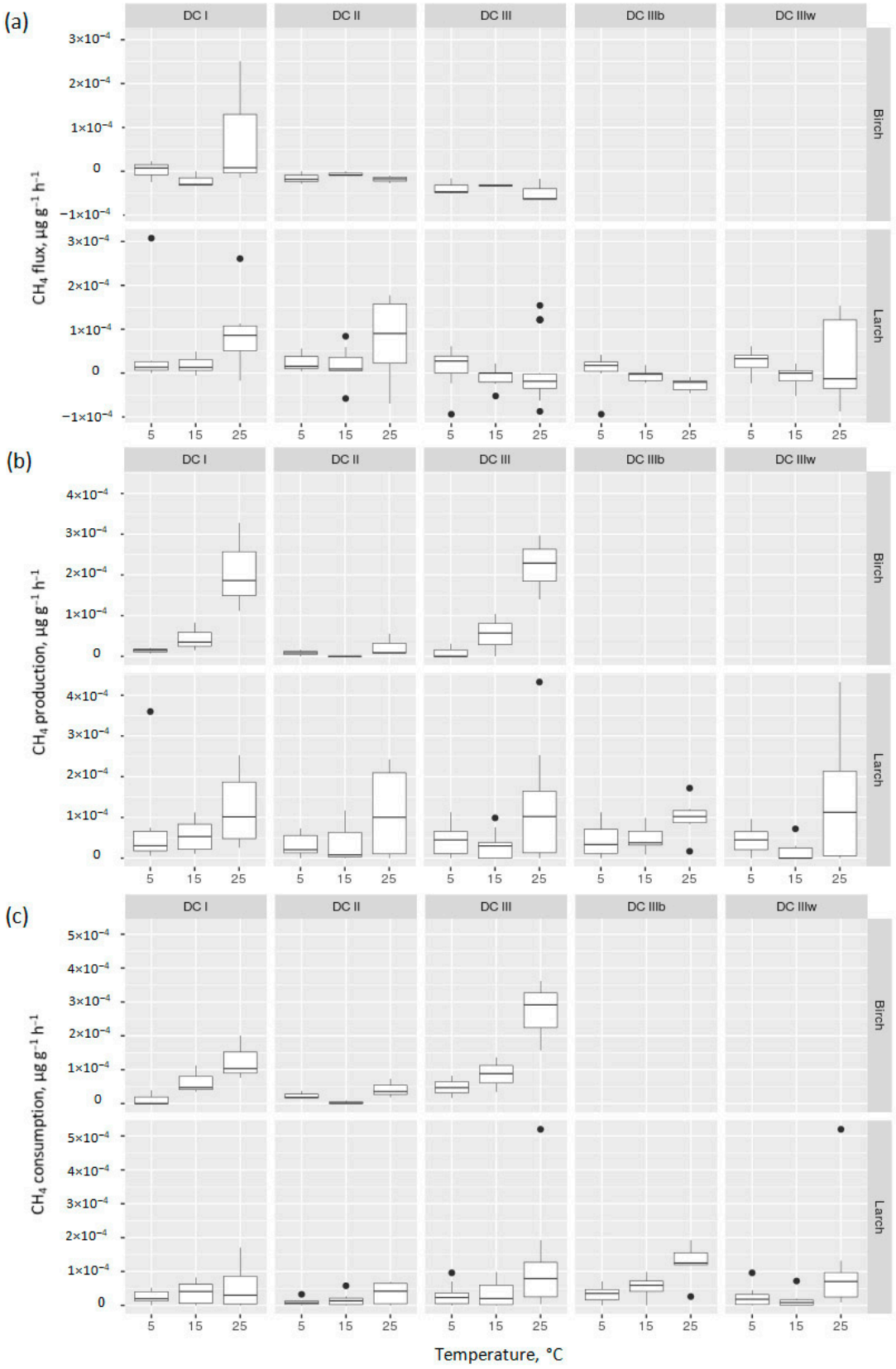

Figure 2. The rate of CH_4 flux (**a**), CH_4 production (**b**) and CH_4 consumption (**c**) during decomposition of larch (Larch) and birch (Birch) wood shown as box plots: DC I–DC III—decomposition classes I–III; DC IIIw—separately larch wood of DC III decomposed by white rot fungi; DC IIIb—separately larch wood of DC III decomposed by brown rot. CH_4 consumption (**c**) was calculated as a difference between CH_4 production (**b**) and CH_4 flux (**a**).

During exposition of larch CWD at +5 °C the average flux of CH_4 decreased strongly from DC I to DC II, and from DC II to DC III decomposed by brown rot (from $6.14 \times 10^{-5} \pm 3.36 \times 10^{-5}$ μg CH_4 g^{-1} h^{-1} to $2.27 \times 10^{-5} \pm 0.69 \times 10^{-5}$, and to $1.67 \times 10^{-6} \pm 1.32 \times 10^{-6}$ μg CH_4 g^{-1} h^{-1}, respectively). During exposition at +15 °C the average rate of CH_4 flux did not change noticeably for DC I and DC II. CWD at DC III showed evident increase of CH_4 oxidizing (the average rate of CH_4 flux decreased to $-7.81 \times 10^{-6} \pm 0.35 \times 10^{-5}$ and $-4.99 \times 10^{-6} \pm 0.45 \times 10^{-5}$ μg CH_4 g^{-1} h^{-1} for wood decomposed by white rot and brown rot, respectively). Incubation at +25 °C showed an increasing CH_4 flux from DC I and DC II. Concerning DC III, the methane flux from CWD increased in some cases of white rot decomposition. In contrast, larch CWD decomposed by brown rot showed an increase of the methane oxidizing rate (the average rate of CH_4 flux decreased to $-2.6 \times 10^{-5} \pm 0.51 \times 10^{-5}$ μg CH_4 g^{-1} h^{-1}).

Incubation of birch CWD demonstrated evident methane flux only for DC I. The average rate of this flux increased more than forty folds during incubation at +5 and +25 °C (from $2.01 \times 10^{-6} \pm 1.02 \times 10^{-5}$ to $8.14 \times 10^{-5} \pm 6.53 \times 10^{-5}$ μg CH_4 g^{-1} h^{-1}, respectively). Birch wood at DC II and DC III showed methane oxidation during incubation at all temperatures (Figure 2).

During incubation, $\delta^{13}C$ of CH_4 increased from initial −50–−54‰ up to +60.2–+74.0‰. CWD samples that emitted CH_4 showed a linear relationship between the increase of $^{12}CH_4$ and $^{13}CH_4$ concentrations in the experimental boxes (Figure 3). However, CWD from birch at DC II and from both tree species at DC III showed the decrease or no changes in the $^{12}CH_4$ concentration during incubation. However, for these samples, we observed the significant increase of $\delta^{13}C$ of CH_4 due to evident rising of $^{13}CH_4$ concentration (Figure 3).

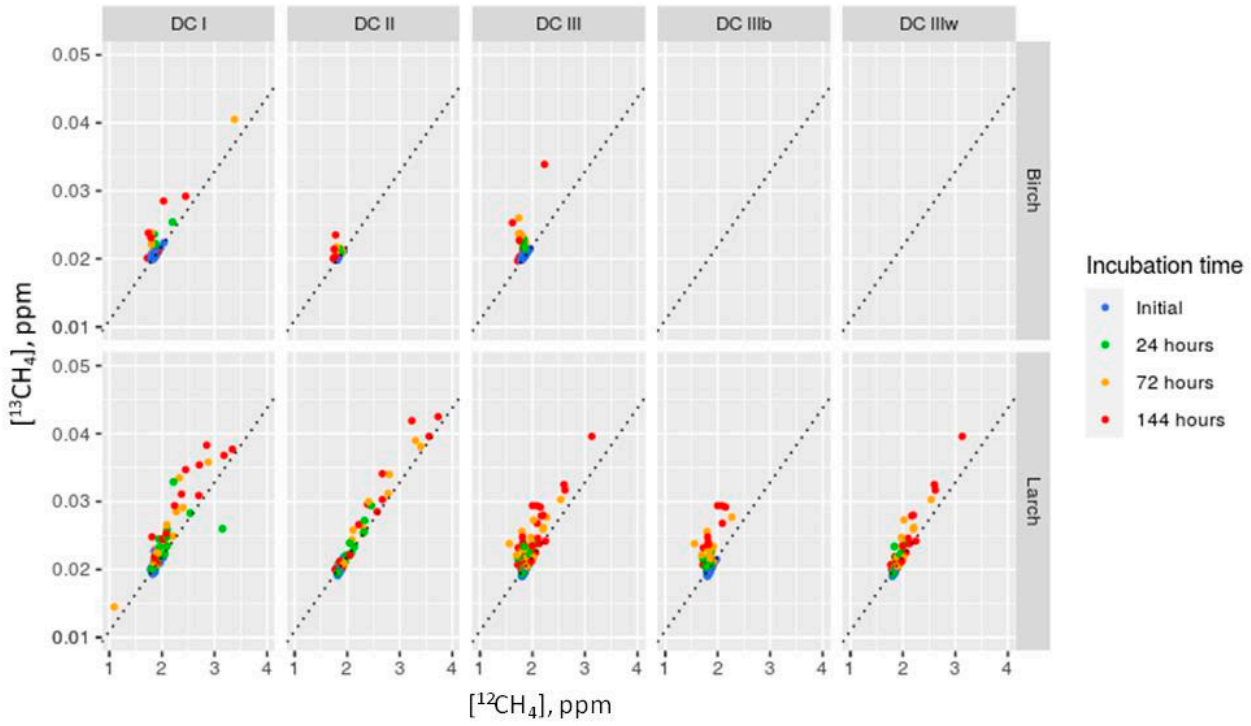

Figure 3. The relationship between $^{12}CH_4$ ($[^{12}CH_4]$, ppm) and $^{13}CH_4$ ($[^{13}CH_4]$, ppm) content during incubation of larch and birch CWD: DC I–DC III—decomposition Classes; DC IIIb—CWD of Decomposition Class III decomposed by brown rot fungi; DC IIIw—CWD of Decomposition Class III decomposed by white rot fungi. Dotted line indicates reference ratio between $^{13}CH_4$ and $^{12}CH_4$ if to assume that $\delta^{13}C$ in the produced methane is similar to that in the substrate (decomposing wood).

Based on the changes of the absolute $^{13}CH_4$ concentration in the headspace of the experimental boxes during CWD incubation, we calculated the possible rate of $^{12}CH_4$ pro-

duction, supposing that carbon isotopic ratio in the produced methane should be similar to that in the substrate—decomposing wood (Table 1). The calculated rate of CH_4 production in all cases exceeded the measured rate of CH_4 flux and showed a significant dependance on temperature (Figure 2b). Based on the difference between rates of calculated methane production and measured methane flux, we assessed the rate of methane consumption (Figure 2c). The average rate of methane consumption increased from DC I to DC III for CWD of both studied tree species. Exception was DC II, which demonstrated the low rate of CH_4 consumption for both species at temperatures of +15 and +25 °C.

3.4. Temperature Sensitivity and Temperature Response of CO_2 and CH_4 Fluxes

To characterize the dependence of CO_2 and CH_4 fluxes on temperature we calculated coefficient Q_{10} for the temperature intervals +5 to +15 °C and +15 to +25 °C. For the CO_2 fluxes from larch wood at early stages of decomposition (DC I and II), the average Q_{10} values were larger for temperature interval from +5 to +15 °C (2.87 ± 0.74 for DC 1 and 3.51 ± 1.85 for DC II) than for +15 to +25 °C (2.33 ± 0.62 for DC I and 2.41 ± 0.97 for DC II). At DC III, the average Q_{10} for CO_2 fluxes from CWD was almost similar within both temperature intervals (3.16 ± 1.62 and 3.11 ± 1.23). Temperature sensitivity was quite different for CWD decomposed by white and brown rot fungi. For CWD decomposed by white rot, Q_{10} for the temperature interval +5 to +15 °C appeared to be lower than that for the interval +15 to +25 °C (1.79 ± 0.77 and 4.01 ± 2.45, respectively). On the contrary, CWD decomposed by brown rot indicated higher temperature sensitivity for the lower temperature interval (+5 to +15 °C) in comparison with +15 to +25 °C (the average Q_{10} value was equal to 4.29 ± 2.47 and 2.78 ± 0.82, respectively). However, factorial ANOVA analysis indicated that differences for decomposition classes and temperature intervals mentioned above were not significant due to the wide range of temperature sensitivity of CO_2 flux (Figure S3b).

The average coefficient Q_{10} for CO_2 emission from birch CWD exceeded 3.00 for DC I and DC III (3.17–3.33 and 3.16–3.69 for DC I and III, respectively) (Figure S3a). Temperature sensitivity of CO_2 flux was significantly lower ($p < 0.05$) for DC II, with Q_{10} values of 2.84 ± 0.15 and 2.65 ± 0.23 for temperature intervals +5 to +15 °C and +15 to +25 °C, respectively. Differences in the temperature sensitivity of CO_2 flux between two studied temperature intervals were nonsignificant ($p > 0.05$).

Methane fluxes had higher temperature sensitivity (Q_{10}) in the temperature interval +15 to +25 °C than at the lower temperatures (+5 to +15 °C). Methane flux increased by 30–48% when temperature raised from +5 to +15 °C, while the increase was about four to eight-fold in case of the temperature increase from +15 to +25 °C. The average Q_{10} for the methane production was 1.14–1.68 and 2.28–3.42 for temperature intervals +5 to +15 °C and +15 to +25 °C, respectively. Temperature sensitivity of methane consumption for wood at DC I was similar within both studied temperature intervals. For DC II and DC III, Q_{10} for this flux increased from temperature intervals +5 to +15 °C to +15 to +25 °C (from 1.16–1.76 to 2.42–2.72, respectively) (Figure S3).

Decomposition class and temperature interval significantly influenced Q_{10} for methane flux and methane production during decomposition of larch and birch wood ($p < 0.05$). For birch wood, Q_{10} of methane consumption also significantly depended on a temperature interval ($p < 0.05$).

Calculated temperature response of CO_2 flux was 0.15–3.12 μg g^{-1} h^{-1} per °C and 0.004–7.64 μg g^{-1} h^{-1} per °C in the temperature interval +5 to +15 °C for birch and larch CWD, respectively. Under the temperatures from +15 to +25 °C, the response increased by 125–258% and 36–124% for birch and larch CWD, respectively (Figure 4). On the average this value was equal to 18.5–32.9% of the CO_2 flux measured at temperature +5 °C, and 13.4–39.1% of the flux at temperature +15 °C.

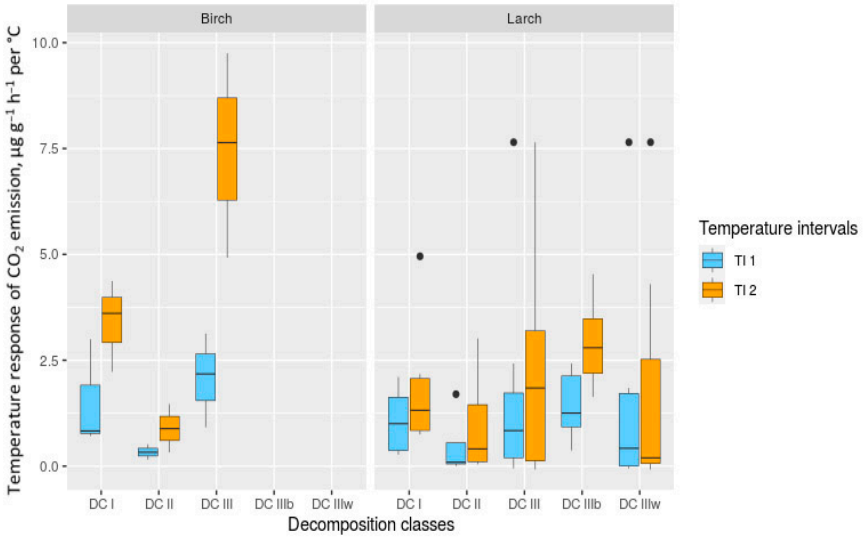

Figure 4. Box plots of temperature response of the CO_2 flux during decomposition of larch and birch CWD at different decomposition classes: TI 1—temperature interval from +5 to +15 °C; TI 2—temperature interval from +15 to +25 °C; DC I–DC III—decomposition classes; DC IIIb and DC IIIw—wood of Decomposition Class III decomposed by brown rot and white rot fungi, respectively.

The average rate of methane flux decreased for the birch CWD at DC I and for the larch CWD at all decomposition classes when temperature increased from +5 to +15 °C, and for the birch CWD at DC II and DC III and for larch CWD decomposed by brown rot in case of the temperature increase from +15 to +25 °C. This reduction was 1.1% and 18.9% per °C in respect to the rate measured at +5 and +15 °C, respectively. In all other cases the rate of CH_4 flux increased with the rise of temperature and this increase was from 5% to 48% of the initial flux rate. The rate of methane production decreased only for DC III for larch and for DC II for birch CWD when the temperature increased from +5 to +15 °C. The average rate of this decline was 8.3% and 12.4% from the flux rate at temperature +5 °C. All other DC of larch and birch CWD showed respective increase of methane production with temperature rise from +5 to +15 °C (0–6.9% and 10.0–38.9%). With the temperature rising from +15 to +25 °C methane production increased by 12.8–46.3% and 24.3–53.8% per each °C for larch and birch CWD, respectively. Methane consumption decreased with temperature increasing only for DC II of birch CWD at the lower temperature interval. The rate of this process declined by 5% per °C. Larch wood at all decomposition classes and birch wood at DC I and DC III showed 2.1–25.7% increase of methane consumption per each °C increment when temperature increased from +5 to +15 °C, and 4.3–145% increment per each °C while temperature kept rising from +15 to +25 °C.

3.5. Effect of Water Content on CO_2 and CH_4 Fluxes

In our study, we analyzed CO_2 and CH_4 fluxes from decomposing CWD at their natural moisture. Water content in these samples varied from 14% to 176% of the mass of the dry wood for different stages of decomposition for larch CWD, and from 88% to 560% of the mass of the dry wood for birch CWD. Variations in CO_2 and CH_4 fluxes from these samples were connected with water content in CWD samples. However, the dependence of these fluxes on wood moisture was nonlinear (Figure 5). The respiration rate of larch wood was significantly positively related to the moisture of CWD samples when wood moisture was lower than 100% ($R = 0.92 - 0.93$ at temperature +5 °C and +15 °C, and $R = 0.88$ at +25 °C, $p < 0.05$). When moisture exceeded 136%, the CO_2 flux decreased, (Figure 5a). Birch CWD samples had higher water contents than the larch samples, and at DC II they also showed positive relationship between CO_2 and CH_4 fluxes and water content ($R = 0.91 - 0.96$, $p < 0.05$). Water content in decomposed birch wood at DC III

exceeded 300%, and the increase of wood moisture from 320% to 500% showed the strong negative effect on the rate of CO_2 and CH_4 fluxes (Figure 5b).

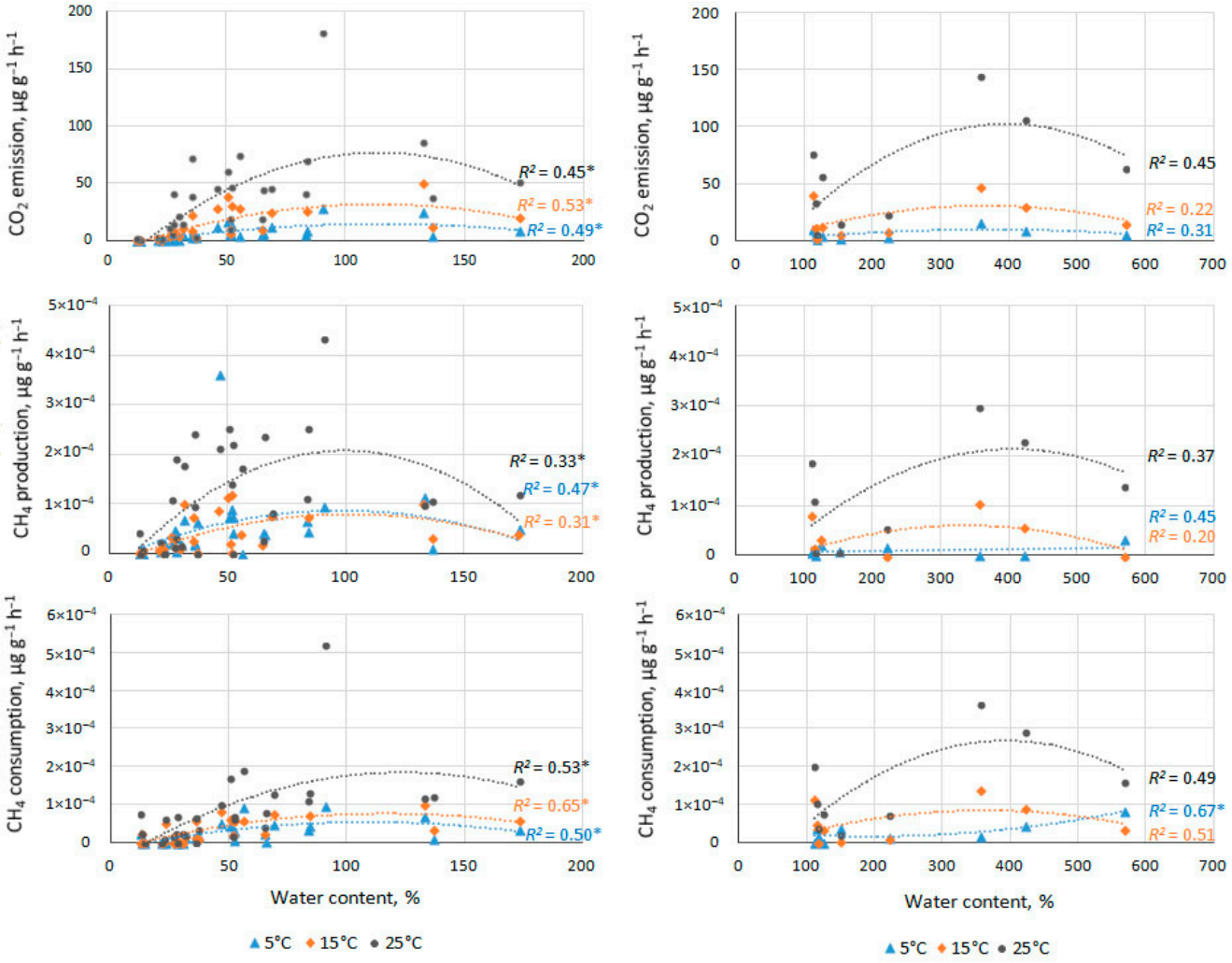

Figure 5. The relationship between CO_2 and CH_4 fluxes and water content of larch (**a**) and birch (**b**) CWD samples at different temperatures. Superscript * indicates significance at $p < 0.05$.

Quadratic regression revealed that 45% to 53% of the CO_2 flux variance, and more than 50% of the variance of CH_4 consumption rate during decomposition of larch CWD, can be explained by the water content in the wood ($p < 0.05$). Methane production also depended on water content in the CWD samples; however, this relation was weaker than for CO_2 and methane consumption ($R^2 = 0.33$–0.47, $p < 0.05$) (Figure 5a).

The measured flux of CH_4 did not depend on water content in the CWD of both tree species. For birch CWD, the water content had a significant influence on the methane consumption rate at the temperature of +5 °C only (Figure 5b). In all the other cases the dependence on the water content was not significant.

3.6. Analysis of The Main Factors Affecting on CO_2 and CH_4 Fluxes

One-way ANOVA test showed that temperature alone was a significant factor for CO_2 flux from decomposing CWD, but it explained only 26% of respiration variance ($R^2 = 0.26$, $p < 0.01$). Temperature together with wood moisture explained 47% of variance for larch wood and 55% of the variance for birch wood (($R^2 = 0.47$, $p < 0.01$) and $R^2 = 0.55$,

$p < 0.05$, respectively). If we add to the model other influencing factors (tree species and decomposition class), it explains 62% of total variance of the respiration rate ($R^2 = 0.62$, $p < 0.05$) (Table S1). Separately for larch wood, these factors explained 51% of the variance of the respiration rate ($R^2 = 0.51$, $p < 0.05$), and 92% for birch wood respiration ($R^2 = 0.92$, $p < 0.05$) (Table S2).

Measured fluxes of CH_4 significantly differed for the two studied tree species ($p < 0.05$). Species and decomposition class were the main influential factors for the CH_4 flux from decomposed wood. All together they contributed about 24% to the total variance of this CH_4 flux ($R^2 = 0.33$, $p < 0.05$) (Table S1).

The calculated rate of CH_4 production significantly depended on the temperature ($R^2 = 0.20$, $p < 0.01$). ANCOVA analysis showed that water content, decomposition class and wood density together with temperature contributed about 44% to the total variance of this process. Temperature alone explained 15% and 45% of total variance of the rate of CH_4 production by decomposing larch and birch wood, respectively ($p < 0.01$) (Table S2). Altogether, temperature, decomposition class, water content, and wood density explained 44% of the variance of the methane production rate for larch wood (Table S2). Significant factors for the rate of CH_4 production during decomposition of birch wood were decomposition class, temperature and their interaction ($p < 0.05$). Altogether they explained almost 80% of the CH_4 production rate variance ($R^2 = 0.79$) (Table S2).

The rate of CH_4 consumption significantly depended on tree species, decomposition class, temperature, and their interaction ($R^2 = 0.41$, $p < 0.01$). Temperature alone explained only about 15% of total variance of the CH_4 consumption rate ($R = 0.38$, $p < 0.01$). (Table S1). Separately for larch CWD, temperature explained only about 10% of the CH_4 consumption flux variance ($R^2 = 0.10$, $p < 0.05$). Within all variables, the most influential for this flux was the water content. It contributed more than 20% ($p < 0.01$) to the total variance explanation ($R^2 = 0.44$, $p< 0.05$) (Table S2). For birch CWD, temperature alone explained 34% of variance of the methane consumption flux ($p < 0.01$). Together with other variables, the predictive capacity of the model reached 86% and the most significant factors of this model were temperature (39.9%, $p < 0.01$) (Table S2).

The rate of measured flux of CH_4 from decomposing wood had no correlation with CO_2 flux, while the calculated rate of CH_4 production was significantly ($p < 0.05$) correlated with the rate of CO_2 emission ($R = 0.75$ and 0.89 for larch and birch wood, respectively) (Figure 6). The rate of methane consumption also had a strong correlation with the rate of CO_2 flux both for larch and for birch CWD ($R = 0.81$, $p < 0.05$ and $R = 0.96$, $p < 0.05$, respectively) (Figure 6). CO_2 flux contributed 35% to the explained variance of the methane production rate ($p < 0.01$), and 51% to the total CH_4 consumption variance described by all factors (Table S3).

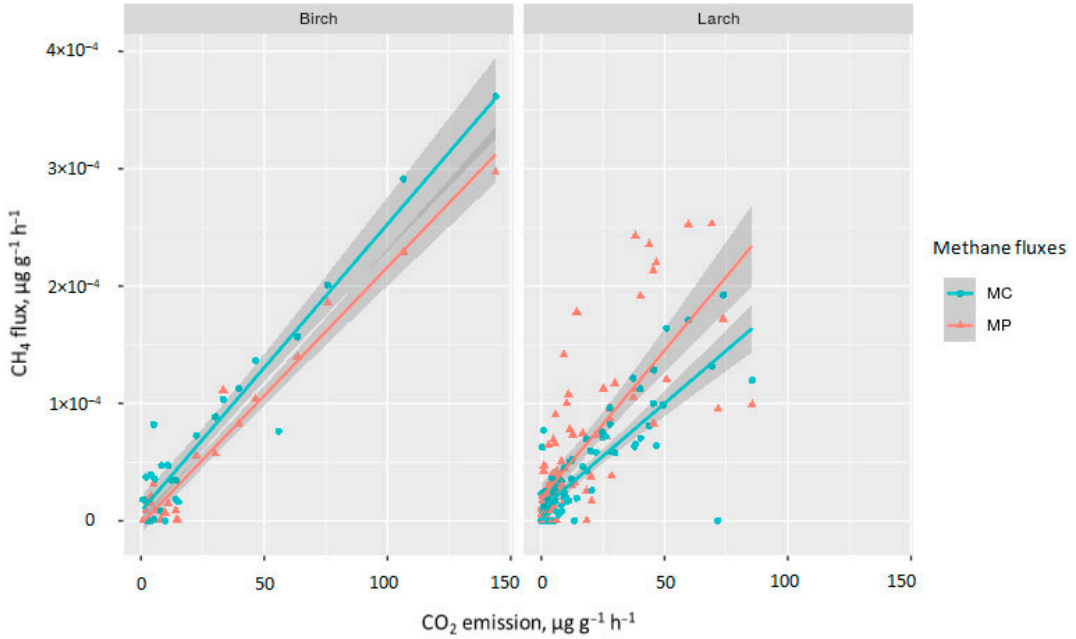

Figure 6. The relationship between CO_2 emission and CH_4 fluxes during decomposition of birch and larch CWD samples: MP—methane production, MC—methane consumption. Shadowed area indicates the 95% confidence interval of the trend line.

3.7. Effect of The Main Factors on Temperature Sensitivity (Q_{10}) and Temperature Response of CO_2 and CH_4 Fluxes

Temperature coefficient Q_{10} for CO_2 and CH_4 fluxes did not differ significantly for the two studied tree species. However, ANOVA analysis showed that temperature sensitivity of CH_4 production significantly differed ($p < 0.01$) for the two studied temperature intervals. Temperature sensitivity of CO_2 flux significantly depended on moisture of CWD (6.7% of variance, $p < 0.05$). Within the lower temperature interval (from +5 to +15 °C) temperature sensitivity of CH_4 consumption significantly depended on interaction between tree species and decomposition class ($p < 0.05$).

Separately for larch CWD, the temperature interval explained 14% and 20.4% of Q_{10} variance for CH_4 production and CH_4 flux ($p < 0.05$), respectively. Temperature sensitivity of CH_4 production depended also on decomposition class (15.4% of total variance of Q_{10}, $p < 0.05$). Temperature sensitivity of CO_2 flux significantly depended on water content (23.5% of variance, $p < 0.05$), decomposition class (13.5% of total variance, $p < 0.01$), and interaction between decomposition class and temperature interval (18.5% of total variance, $p < 0.01$).

Within the lower temperature interval (from +5 to +15 °C), the temperature sensitivity of CO_2 flux mainly depended on decomposition class (45.7% of total variance, $p < 0.05$), while under the higher temperature interval (from +15 to +25 °C), the main factor was moisture (48.3% of total variance, $p < 0.01$). Under the lower temperatures (from +5 to +15 °C), the Q_{10} for methane consumption significantly depended on decomposition class, mass, and volume of the sample. These factors and covariates contributed 31.3%, 25.4%, and 18.3%, respectively, to the explanation of total variance ($p < 0.05$).

Temperature sensitivity of CO_2 and CH_4 fluxes from birch wood had no significant dependence on studied factors and covariates.

The temperature response of the CO_2 and CH_4 fluxes calculated from a linear model significantly ($p < 0.05$) differed for studied temperature intervals (from +5 to +15 °C and from +15 to +25 °C). Tree species influenced only temperature response of CO_2 and CH_4 production ($p < 0.05$), and temperature response of CH_4 flux and CH_4 consumption did not differ for the two studied species. Within the separate temperature intervals, the main factor influencing temperature response of CO_2 flux was the water content in the wood

(42% and 30% to the total explained variance at the temperature intervals from +5 to +15 °C and from +15 to +25 °C, respectively, $p < 0.05$). Decomposition class of CWD additionally contributed 16% and 22% ($p < 0.05$).

Temperature response of measured CH_4 flux did not depend on any of studied parameters. In addition, temperature response of calculated CH_4 production did not show any significant difference in the temperature interval from +5 to +15 °C, but depended on decomposition classes at the interval between +15 and +25 °C ($p < 0.05$). Decomposition class as well significantly influenced the temperature response of CH_4 consumption when temperature increased from +5 to +15 °C (17% of variance, $p < 0.05$). The second significant factor was the water content (13.5% of variance, $p < 0.05$). Effect of moisture of CWD samples significantly increased in the temperature interval from +15 to +25 °C, and the water content explained more than 23% of variation in temperature response of the methane consumption ($p < 0.05$).

Separately for larch CWD, the water content explained 30% of temperature response of CO_2 flux at lower temperature interval (from +5 to +15 °C) and only 13% under the higher temperatures (from +15 to +25 °C). Temperature response of CH_4 fluxes mainly depended on decomposition class or density of wood in both temperature intervals. The main factor influencing temperature response of CO_2 and CH_4 fluxes from decomposing birch CWD was decomposition class, which explained from 46% to 83% of total variance in temperature response of this fluxes ($p < 0.05$).

4. Discussion

4.1. CO_2 and CH_4 Fluxes from Decomposing CWD

The rate of CO_2 emission from CWD samples was higher at DC I than at DC II for CWD from both tree species; however, for larch this difference was not significant at $p < 0.05$. The lower rate of respiration of logs at DC II can be a consequence of soluble sugars, starch, and non-structural carbohydrates depletion in decomposing wood [68]. Microorganisms consume these substrates at first. In addition, the wood-decaying fungi, which are the main decomposers of cellulose and lignin, do not invade widely into the solid wood at DC I. At DC III, the wood density decreased significantly and fungi and bacteria are able to penetrate the wood. Larger fungal and microbial biomass and resulting activity in wood at the advanced stages of decomposition lead to the higher respiration rates. Additionally, wood decomposition is accompanied by a relative nitrogen enrichment [69–74], which can promote decomposition rate of initially nitrogen-poor substrate [4,75,76].

Deciduous and coniferous wood differ in terms of morphology and chemical composition of the cell wall. Higher decomposition rates of deciduous wood correspond with their lower lignin concentration and higher nutrient concentrations in comparison with coniferous wood [4,76,77]. However, in our experiment, birch wood produced the significantly higher rate of CO_2 emission than larch only at the late decomposition stage under the highest temperature +25 °C. In other cases, CO_2 emissions from larch and birch CWD were comparable despite the higher nitrogen content and lower C to N ratio in the birch wood (Table 1). It could be a consequence of high water content in the birch wood that will be discussed below.

During incubation, we observed significant increasing of δ^{13}C-CH_4 (up to +60.2–+74.0‰) and rising of the absolute concentration of $^{13}CH_4$ in the headspace of the experimental boxes. The similar ^{13}C-CH_4 enrichment (from initial δ^{13}C-CH_4 equal to -37.8 ± 0.6‰ to $+84.6 \pm 0.4$‰) was observed in the incubation experiment on anaerobic oxidation of methane by *Methylomirabilis oxyfera* [78], and during aerobic microbial oxidation of CH_4 (from −22.0 to +76.4‰) in closed isotopic system [79]. These authors also showed that the progressive isotope enrichment was identical in all the cases independently on absolute biomass and methane content.

Light fraction of CH_4 ($^{12}CH_4$) is easier oxidized in comparison with methane containing a heavier carbon isotope ($^{13}CH_4$) [51–53], so that the latter can relatively increase in the experimental air volume, shifting δ^{13}C-CH_4. Increase of the absolute concentration of

$^{13}CH_4$ in the headspace of the experimental boxes indicated evident methane production during decomposition of studied CWD. An increase of the absolute concentration of $^{13}CH_4$ was observed in both cases when the concentration of $^{12}CH_4$ decreased due to methane oxidation processes and when content of $^{12}CH_4$ did not change or increase. We did not observe any changes of $^{13}CH_4$ concentration in the control boxes with and without water, so we concluded that production of this gas was related with decomposition of studied CWD samples.

We propose that methane produced inside wood could be oxidized by methanotrophs in wood pores. Because methanotrophs preferentially oxidize $^{12}CH_4$, then mainly $^{13}CH_4$ could reach the wood surface and go out to the headspace of the experimental box. As a result, headspace air in the box becomes enriched with $^{13}CH_4$ even if the content of $^{12}CH_4$ did not change (in the case if produced $^{12}CH_4$ was completely consumed inside wood) (e.g., birch CWD at DC II in Figure 3).

In some cases, when the rate of methane production is high or if there are not many methanotrophs in decomposed wood, some part of the produced $^{12}CH_4$ could also reach the wood surface and air around. In this case, we observed an increase of absolute concentrations both of $^{13}CH_4$ and $^{12}CH_4$ (e.g., larch CWD at all DCs and birch CWD of DC I in Figure 3). However, in this case, the isotope ratio in methane also can be enriched with ^{13}C due to the fact that some part of produced $^{12}CH_4$ is consumed inside the wood anyway.

In other cases, high activity of methanotrophs can lead to the oxidation of $^{12}CH_4$ in the air of the headspace. In these cases, we observed an evident decrease of total methane content in the headspace of experimental boxes. However, at the same time, flux of $^{13}CH_4$ from decomposing wood, like that described above in the first case, could exist. This can result to a stronger enrichment with $^{13}CH_4$ than would be expected in the case of simple methane consumption from the air or increase of the absolute concentration of $^{13}CH_4$ (e.g., birch CWD at DC III in Figure 3).

We assessed the rate of methane production and methane consumption based on the assumption that evolved $^{13}CH_4$ reflects the rate of methane production due to its discrimination by methanotrophs.

Methane flux was higher at early decomposition stage in contrast to methane consumption that increased from DCI to DCIII for both tree species. Decreasing wood density and enrichment of CWD in nitrogen promote the increase of fungal and bacteria species richness at the advanced stages of decomposition [80]. In addition, as it was reported by Mäkipää with co-authors [81], the highest number of methanotrophs were found just in the late stage of decomposition. The methane production and methane consumption rates in most cases were higher for birch CWD than for larch, probably due to different fungal communities decomposing wood of these tree species [82].

Our incubation experiment demonstrated that, for both tree species, the stage of decomposition influenced the rate of CO_2 and CH_4 fluxes from decomposing wood and their temperature sensitivity and temperature response. Similar results were reported by Herrmann and Bauhus [83]. They studied temperature effect on CO_2 flux from decomposing CWD of three tree species and found that about 80% of the variation in respiration could be explained by species, wood density and moisture. In our study, wood density decreased from DC I to DC III (Table 1) and these classes showed different rates of CO_2 emission and different temperature sensitivity. Other studies also reported a significant effect of wood density on mineralization flux from CWD [55,56,60,61,84].

The strong positive correlation between CH_4 production rates and CO_2 emission indicated evident strong relationship of this flux with biological activity of decomposers in the dead wood. The significant strong relationship between CO_2 flux and CH_4 consumption is also a sign that oxidation of methane in decomposing wood is an active biological process. One of the products of CH_4 oxidation is CO_2; however, the rate of methane oxidation does not propose significant contribution of this flux to the total respiration. The calculated rate of CH_4 consumption is less than 0.01% of the total rate of CO_2 emission, so it did not significantly influence on the CO_2 efflux.

Methane flux from decomposing coarse woody debris was reported by numbers of authors [31–36]. They proposed that the main organisms responsible for this flux could be methanogenic bacteria and archaea that could survive in decomposing CWD due to the anaerobic conditions inside wood or that tree stems serve as a tube to release methane produced in the soil. In our study, CH_4 production was closely correlated to the rate of CO_2 emission, indicating a biological source of this flux and connection with activity of aerobic organisms. Evidence of aerobic methane production by wood-decaying fungi was reported earlier [39]. Our results showed that aerobic methane production is probably the main process contributing to the methane flux from decomposing coarse woody debris, because CH_4 fluxes had negative relation with oxygen deficit caused by high water content in decomposed wood.

Comparison with the rate of CO_2 emission from the soils of the studied region [85,86] indicated that CO_2 flux from the stock of decomposing CWD could comprise 2–5% of soil CO_2 efflux in forests undisturbed by fire during more than 100 years. Whereas, already one year after the fire, it increases significantly due to both the decrease in soil respiration and the increase in dead wood stock, reaching 82–139% of the soil flux. Methane emission from soil surface in these northern boreal larch forests was reported to be equal to 0.25–3.35 μg CH_4 m^{-2} h^{-2} [87]. Calculated possible CH_4 flux from existing CWD stock in old-growth and mature larch forests [19,85] can comprise 2–40% of the soil methane emission. In their research, Köster et al. [85] have found out that soil of all the studied postfire ecosystems (from 1 to >100 years after the fire) acted as a CH_4 sink. It means that CWD could be the only source of CH_4 in such ecosystems.

4.2. Effect of Water Content on CO_2 and CH_4 Fluxes

Water content in the wood was one of the most significant drivers of CO_2 and CH_4 fluxes in our experiment. Moisture availability is an important control of decomposer activity [88,89]. Water content affects the fungi inhabiting wood, influencing their growth and decay rates and the outcome of mycelial interactions [90–92]. Moisture is mentioned as a significant determinant of extracellular hydrolytic and oxidative enzyme activity [93–95]. The optimal and maximum values of wood moisture for decomposer activity are highly variable. For example, wood with the moisture content of 60–130% reported to decay rapidly; 90–120% may be the top limit for some decay fungi [96,97]; however, optimum values between 160–180% have been found for others [96]. Moisture content in the wood in our experiment varied significantly (from 14% to 560%), and for some samples it was lower than fiber saturation point (i.e., lower than 24–31% of dry weight) [96,98]. Consequently, these samples showed the extremely low rate of CO_2 and CH_4 fluxes. The dependence of CO_2 flux on the water content in the wood was unimodal—it peaked at intermediate water content and declined following increasing moisture, probably due to the rising of oxygen deficiency. It is interesting that methane flux and methane production also decreased under the high water content, despite that they should not depend on oxygen availability, but rather they should increase under the anaerobic conditions [37].

In our study, we analyzed CO_2 and CH_4 production from decomposing CWD at field moisture. Birch CWD samples had higher water content than larch wood, which could be attributed to the species features, because larch and birch CWD samples were taken at the one plot and at the same time, but they had quite different moisture due to the tree species peculiarities. Bulk density of the wood is considered to be a significant factor influencing water content, due to the increase of the water holding capacity of the wood with a decrease in density [99]. For our samples, water content strongly depended on bulk density only for birch wood, in contrast to larch wood that had the similar bulk density but significantly lower water content (Figure 7).

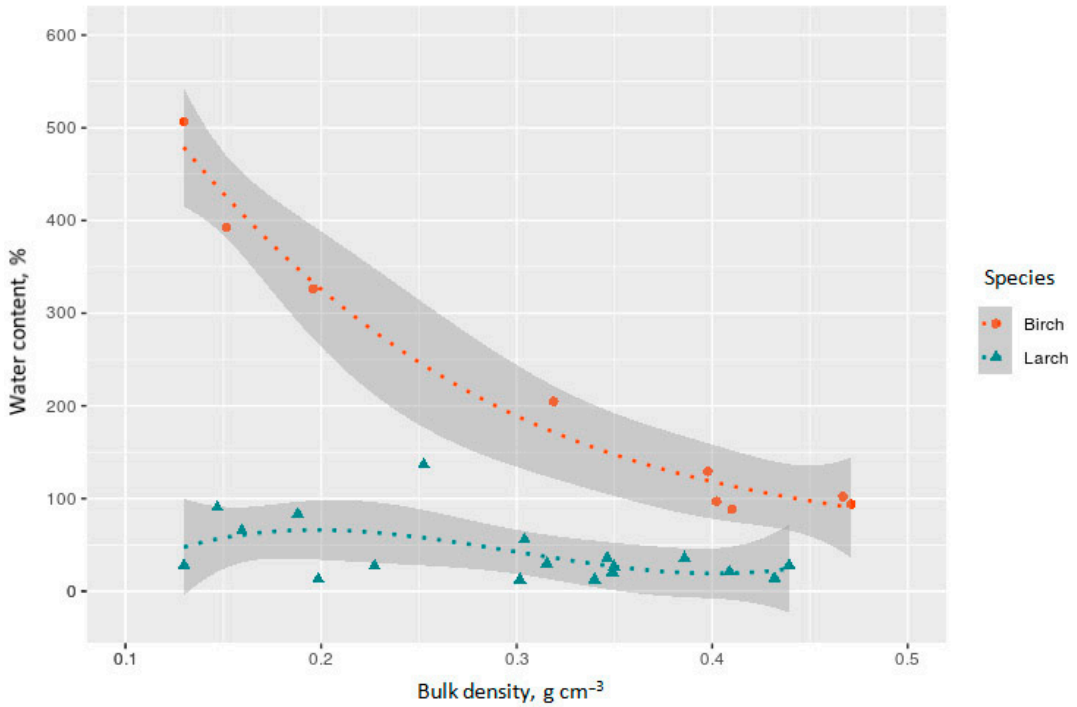

Figure 7. The relationship between bulk density and water content in the decomposed larch and birch wood. Shadowed area indicates the 95% confidence interval of the smooth line.

The peculiarity of birch logs lies in their strong and water-resistant bark, which remains on the log during the whole period of wood decomposition. This bark prevents wood inside the log from drying and provides a high level of wood moisture especially at the late stages of decomposition. It is possible that the community of birch wood decomposers (microorganisms and fungi) are well adapted to the partly anaerobic conditions inside overwetted wood, which may explain the high rate of respiration at a water content of more than 300% of dry weight. The rate of CO_2 emission from birch CWD decreased only at a moisture level exceeding 320%, while respiration flux from larch wood dropped already at significantly lower moisture (136%).

As it was found in the earlier studies, water content and temperature interactions could explain 61–80% of the observed variation in CO_2 flux from decomposing CWD [55,56,59,61,83,100,101]. In our study, interaction of temperature and moisture explained only 35% of respiration flux. However, moisture effect was stronger for larch wood, which had low water content and, probably, its decomposition was water limited. The most influential factors for birch wood respiration were temperature and decomposition class.

4.3. Temperature Sensitivity of CO_2 Flux

Low initial content of easily decomposable organic substances in wood [102] cannot suppose significant effect of this component on the rate of CO_2 and CH_4 fluxes during 20 days experiment especially for the late decomposition stages of CWD. It means that changes in the rate of CO_2 and CH_4 production at different temperatures can be attributed to the temperature effect on these fluxes. The Q_{10} values calculated from measured CO_2 emission, under the temperature between +5 to +15° C in our study (2.87–3.51 for larch and 3.17–3.33 for birch), are comparable to the Q_{10} values reported for coniferous (Korean pine) and deciduous (Amur linden) logs investigated by Wu et al. [60] (2.41–2.75 and 2.55–2.95, respectively). Yatskov et al. [77] also reported the stronger effect of temperature on the decomposition rate of CWD for birch (*Betula pendula*) as for coniferous tree species with more decay-resistant heartwood. For CWD in a European beech forest in Central Germany, Q_{10} values of 2.2–2.7 for decay stages one to four were observed between temperatures of 0 and +20 °C [83]. For deciduous species in Michigan, USA [103], and for the conifer *Picea*

mariana in Manitoba, Canada [55], Q_{10} values of 2.20–2.57 were reported. The temperature sensitivity of CO_2 flux from CWD of pine, elm and oak logs in Southern Primorye, Russia, was 2.41, 1.89, and 2.28, respectively [104]. Based on the analysis of a global data set comprising the CWD decay rates and average annual temperatures, Mackensen et al. [105] showed the average Q_{10} value equal to 2.53.

Non-linear temperature dependency of CWD respiration was also observed in many previous studies [56,60,61,83,100,103]. The exponential model was only applicable for temperatures below +22 °C. A decreasing temperature sensitivity with rising temperatures above +20 °C was observed in a laboratory incubation study by Wang et al. [55] and in field measurements of CWD respiration by Gough et al. [103]. The lower rate of Q_{10} increase, nearly reaching a stable state, was shown as the temperatures increased from +18 to +36 °C. Consequently, Yoon et al. [58] proposed that the logistic model should be used to better describe the response of CWD respiration to temperature change. They also presumed that the decrease of temperature sensitivity of CWD respiration at high temperatures might have been caused by water loss under high temperature incubation.

In our study, the Q_{10} value for CO_2 flux was smaller at the temperature interval from +15 to +25 °C as compared to that from +5 to +15 °C only for larch wood at DC I and II, and did not change for DC III. It means that for DC III the respiration rate did not reach a plateau at +25 °C, but continued to increase, despite that moisture of these samples varied widely, from very low 12.5–27.8% for wood decomposed by the white rot to higher values for samples decomposed by brown rot (29.8–136%).

Birch wood at DC I showed a decreasing Q_{10} from lower to higher temperature intervals, the similar values of Q_{10} for studied temperature intervals were observed for DC II. The late stage of decomposition (DC III) showed increasing Q_{10} at higher temperatures. Such different patterns of temperature sensitivity changes probably reflect a succession of the decomposer community during decomposition of the wood. A similar increase of temperature sensitivity within the higher temperature interval was observed for larch wood at DC III decomposed by white rot. Temperature sensitivity of wood decomposed by brown rot decreased from lower to higher temperature intervals. Probably, decomposition of carbohydrates requires lower activation energy in comparison with lignin degradation [106]. Both tree species showed higher temperature sensitivity at lower temperatures at early decomposition stages. At the late decomposition stage, increasing lignin decomposition causes a shift of temperature sensitivity to the higher temperature interval. A similar shift of the respiration maxima at late decomposition stages to the higher temperature, in comparison with earlier decomposition classes, was found by Rinne-Garmston with co-authors [99].

4.4. Temperature Sensitivity and Temperature Response of Methane Fluxes

Methane exchange between decomposing CWD and the atmosphere is a result of two contrary directed processes: methane production and methane consumption. Both of these processes are dependent on temperature. However, the temperature sensitivity of these processes varied independently within two studied temperature intervals, producing differing ratios between the rates of these processes. Temperature coefficient Q_{10} is one of the most common measure of temperature sensitivity. However, Q_{10} is not the rate of change with respect to temperature, but rather the ratio between two rates at different temperatures [29]. Temperature coefficient Q_{10} shows how much the rate of the process is altered with temperature increase by 10 °C. It is; thus, a relative measure that characterizes temperature sensitivity of the process but does not allow for recognition of the shift in ratio between contrary directed processes with temperature change. Additionally, coefficient Q_{10} was not a good measure of temperature sensitivity of CH_4 fluxes, because, in some cases the rate of these fluxes was negative or equal to zero. In such cases, Q_{10} inadequately reflected changes in the rate of CH_4 fluxes. It could be negative even in the case when the rate of the flux was changing from negative to positive or was equal to zero if flux decreased to zero at a higher temperature, or could not be calculated due to division by

zero in case if the flux was equal to zero at a lower temperature. In addition, Q_{10} can show which flux increases faster—CH_4 production or CH_4 consumption. However, Q_{10} fails to show changes in ratio between the absolute rates of these two fluxes and does not allow to assess which CWD sample can emit more methane to the atmosphere [30].

Theoretically, temperature sensitivity is the rate of change in fluxes with respect to temperature [30]. Mathematically, it means that temperature sensitivity is the first derivative of the temperature dependence of studied process [29]. Calculated from the linear model, the temperature response showed how much, on average, the rate of the process changed with each degree of the temperature within the studied temperature interval.

To predict changes of CH_4 flux in respect to temperature change, the absolute values of the temperature response of methane fluxes are more useful than Q_{10} values. The ratio between temperature responses of CH_4 production and methane consumption indicates whether methane flux will increase or decrease. If the temperature response of methane production is higher than that of methane consumption, then the rate of methane flux will increase with respect to temperature increasing (Figure 8).

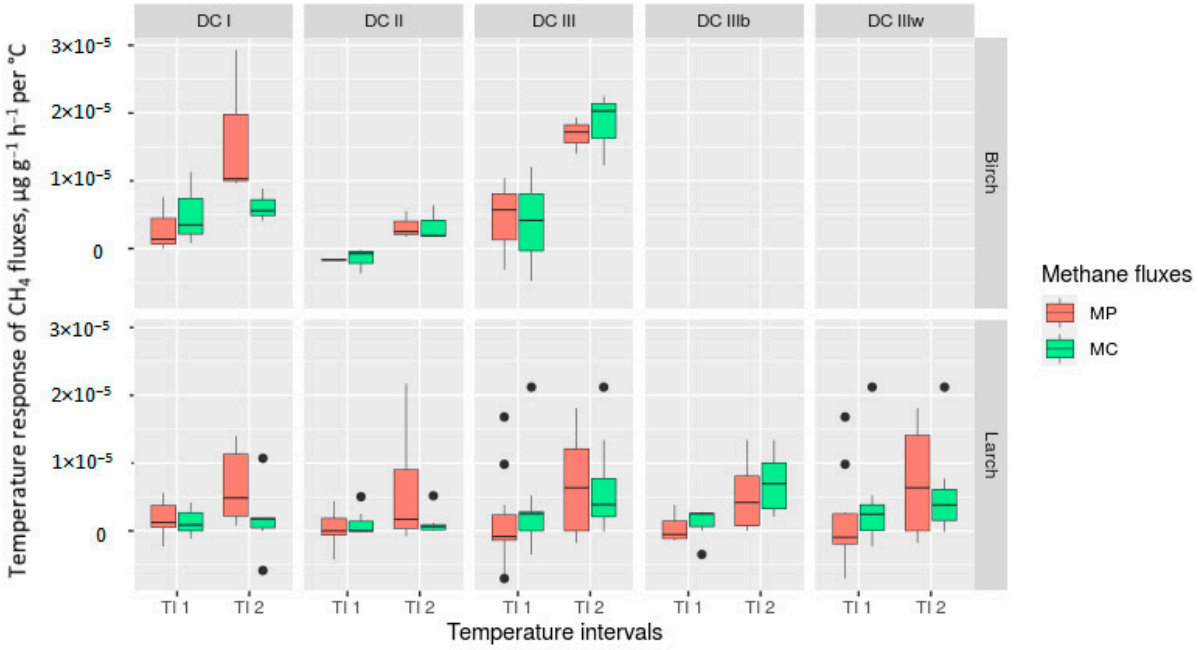

Figure 8. Temperature response of the CH_4 fluxes during decomposition of larch and birch CWD at different decomposition classes: MP—methane production; MC—methane consumption; TI 1—temperature interval from +5 to +15 °C; TI 2—temperature interval from +15 to +25 °C; DC I—DC III—decomposition classes; DC IIIb and DC IIIw—wood of Decomposition Class III decomposed by brown rot and white rot fungi, respectively.

For wood of both tree species at the early stage of decomposition (DC I), the temperature response of methane production was almost twice higher than that of methane consumption under conditions of temperature increase from +15 to +25 °C. This indicates that, in boreal forests, CWD of the early decay stage can serve as a source of methane flux to the atmosphere when air temperatures increase above +15 °C.

5. Conclusions

The results of the incubation experiment showed that CWD of larch and birch in the northern boreal forests can be a source of CH_4 flux to the atmosphere in addition to the CO_2 efflux. This is important because CH_4 is a more active greenhouse gas than CO_2.

According to the IPCC reports and prognoses [11], forest ecosystems in the northern boreal zone are expected to be subjected to a strong increasing temperature due to climate change. Our data suggest that the contribution of CWD to the greenhouse gas fluxes under expected climate changes depends on temperature and precipitation regimes. Increment of

days with temperature above +15 °C can lead to the increase of CO_2 and CH_4 fluxes under conditions where the water content in the wood does not limit decomposition.

The temperature response of CWD respiration and methane production depends on the tree species. Another significant factor influencing CH_4 production and CH_4 consumption is the decomposition class. Disturbances or a general increase of tree death caused by climate change can enlarge the stock of fresh CWD. This can lead to the rise of CH_4 flux to the atmosphere, as CWD at the first stage of decomposition produces and emits the highest amount of CH_4.

We calculated the temperature response of methane fluxes based on the assumption of the linear relationship within the studied temperature intervals covering 10 °C. However, temperature dependence of CH_4 fluxes within these temperature ranges could be nonlinear. We think that additional studies are needed to assess the specificity of the temperature response of CH_4 fluxes within the studied temperature intervals and for a wider range of temperatures, which can be observed in the boreal region and is also expected in relation with prognoses of climate changes.

The results of our experiment showed a strong positive correlation between CH_4 production and CO_2 emission, indicating biological source and supporting findings on the aerobic character of the main process contributing to the CH_4 flux from decomposing coarse woody debris.

Supplementary Materials: The following are available online at https://www.mdpi.com/article/10.3390/f12050624/s1, Figure S1: Cumulative CO_2 production during decomposition of larch wood, Figure S2: Cumulative CO_2 production during decomposition of birch wood, Figure S3: Box plots of temperature coefficient Q_{10} of CO_2 and CH_4 fluxes from birch and larch wood of different classes of decomposition at two temperature intervals, Table S1: Analysis of covariance (ANCOVA) between CO_2 and CH_4 fluxes and the explaining variables in the laboratory incubation experiment, Table S2: Analysis of covariance (ANCOVA) between CO_2 and CH_4 fluxes and the explaining variables separately for decomposition of larch and birch CWD, Table S3: Analysis of covariance (ANCOVA) between CH_4 fluxes and the explaining variables (including rate of CO_2 emission) in the laboratory incubation experiment.

Author Contributions: Conceptualization, L.M.; methodology, L.M.; validation, L.M. and M.M.; formal analysis, L.M.; investigation, L.M. and M.M.; resources, L.K. and M.M.; writing—original draft preparation, L.M.; writing—review and editing, L.M., N.P., M.M., G.G.; visualization, L.M. All authors have read and agreed to the published version of the manuscript.

Funding: The research was funded by RFBR, Krasnoyarsk Territory and Krasnoyarsk Regional Fund of Science, project number 20-44-240008 and by State Assignment of Sukachev Institute of Forest SB RAS (N° 0287-2021-0008).

Data Availability Statement: Data is contained within the article.

Acknowledgments: The authors are grateful to Svetlana Evgrafova for her valuable comments, advices, and remarkable methodological support. We thank two anonymous reviewers for their valuable comments and suggestions, which help to improve this paper.

Conflicts of Interest: The authors declare no conflict of interest.

References

1. NASA GISS: Science Briefs: Greenhouse Gas Influence on Northern Hemisphere Winter Climate Trends. Available online: https://www.giss.nasa.gov/research/briefs/shindell_04/ (accessed on 7 July 2020).
2. Zamolodchikov, D.G.; Utkin, A.I.; Korovin, G.N.; Chestnykh, O.V. Dynamics of Carbon Pools and Fluxes in Russia's Forest Lands. *Russ. J. Ecol.* **2005**, *36*, 291–301. [CrossRef]
3. Harmon, M.E.; Fasth, B.G.; Yatskov, M.; Kastendick, D.; Rock, J.; Woodall, C.W. Release of Coarse Woody Detritus-Related Carbon: A Synthesis across Forest Biomes. *Carbon Balance Manag.* **2020**, *15*, 1–21. [CrossRef] [PubMed]
4. Weedon, J.T.; Cornwell, W.K.; Cornelissen, J.H.C.; Zanne, A.E.; Wirth, C.; Coomes, D.A. Global Meta-Analysis of Wood Decomposition Rates: A Role for Trait Variation among Tree Species? *Ecol. Lett.* **2009**, *12*, 45–56. [CrossRef]
5. Fournier, T.P.; Brossier, B.; Gasssuthier, O.; Carcaillet, C. Post-Fire Dynamics and Spatial Heterogeneity of Woody Debris Associated with Pinus Halepensis in an Oak-Pine Mediterranean Ecosystem. *Écoscience* **2012**, *19*, 356–363. [CrossRef]

6. Mukhortova, L. Carbon Budget Recovery and Role of Coarse Woody Debris in Post-Logging Forest Ecosystems of Southern Siberia. *Bosque* **2012**, *33*, 261–265. [CrossRef]
7. Osone, Y.; Toma, T.; Warsudi; Sutedjo; Sato, T. High Stocks of Coarse Woody Debris in a Tropical Rainforest, East Kalimantan: Coupled Impact of Forest Fires and Selective Logging. *For. Ecol. Manag.* **2016**, *374*, 93–101. [CrossRef]
8. Vedrova, E.F.; Evdokimenko, M.D.; Bezkorovaynaya, I.N.; Mukhortova, L.V.; Cherednikova, Y.S. Reserves of Carbon in the Organic Matter of Postfire Pine Forests in the Southwest of the Baikal Region. *Contemp. Probl. Ecol.* **2012**, *5*, 645–653. [CrossRef]
9. Mukhin, V.A.; Voronin, P.Y. Mycogenic Decomposition of Wood and Carbon Emission in Forest Ecosystems. *Russ. J. Ecol.* **2007**, *38*, 22–26. [CrossRef]
10. Komhyr, W.D.; Gammon, R.H.; Harris, T.B.; Waterman, L.S.; Conway, T.J.; Taylor, W.R.; Thoning, K.W. Global Atmospheric CO_2 Distribution and Variations from 1968–1982 NOAA/GMCC CO_2 Flask Sample Data. *J. Geophys. Res. Atmos.* **1985**, *90*, 5567–5596. [CrossRef]
11. Haines, A. Climate Change 2001: The Scientific Basis. In *Contribution of Working Group 1 to the Third Assessment Report of the Intergovernmental Panel on Climate Change*; Houghton, J.T., Ding, Y., Griggs, D.J., Noguer, M., van der Winden, P.J., Dai, X., Eds.; Cambridge University Press: Cambridge, UK, 2001; p. 881.
12. Pleshikov, F.I.; Vaganov, E.A.; Vedrova, E.F. *Forest Ecosystems of the Yenisey Meridian*; Publishing House of SB RAS: Novosibirsk, Russia, 2002.
13. Abaimov, A.P.; Zyryanova, O.A.; Prokushkin, S.G.; Koike, T.; Matsuura, Y. Forest Ecosystems of the Cryolithic Zone of Siberia: Regional Features, Mechanisms of Stability and Pyrogenic Changes. *Eurasian J. For. Res.* **2000**, *1*, 1–10.
14. Zyryanova, O.A.; Abaimov, A.P.; Daimaru, H.; Matsuura, Y. Floristic Diversity and its Geographical Background in Central Siberia. In *Permafrost Ecosystems: Siberian Larch Forests*; Osawa, A., Zyryanova, O.A., Matsuura, Y., Kajimoto, T., Wein, R.W., Eds.; Ecological Studies; Springer: Dordrecht, The Netherlands, 2010; pp. 17–39. ISBN 978-1-4020-9693-8.
15. Zyryanova, O.A.; Yaborov, V.T.; Tchikhacheva, T.L.; Koike, T.; Kobayashi, M.; Matsuura, Y.; Satoh, F.; Zyryanov, V. The Structure and Biodiversity after Fire Disturbance in Larix Gmelinii (Rupr.). *Eurasian J. For. Res.* **2007**, *10*, 19–29.
16. Koropachinskiy, I.Y. *North Asian Woody Plants: In 2 Volumes*; Publishing House "Geo". Available online: http://www.izdatgeo.ru/index.php?action=book&id=376 (accessed on 23 December 2020).
17. Krivobokov, L.V.; Zverev, A.A.; Mukhortova, L.V. Floristic Characteristics, Types and Ecology of Larch Forests of the Middle Siberia of Northern Boreal Subzone. *Ecol. Saf.* **2015**, *9*, 190–198.
18. Schimel, D.S.; House, J.I.; Hibbard, K.A.; Bousquet, P.; Ciais, P.; Peylin, P.; Braswell, B.H.; Apps, M.J.; Baker, D.; Bondeau, A.; et al. Recent Patterns and Mechanisms of Carbon Exchange by Terrestrial Ecosystems. *Nature* **2001**, *414*, 169–172. [CrossRef] [PubMed]
19. Mukhortova, L.; Trefilova, O.; Krivobokov, L.; Klimchenko, A.; Vedrova, E. Coarse Woody Debris Stock in Forest Ecosystems on Latitudinal Gradient of Central Siberia. *Int. Multidiscip. Sci. GeoConf. SGEM* **2016**, *2*, 495–502.
20. Kajimoto, T.; Osawa, A.; Usoltsev, V.A.; Abaimov, A.P. Biomass and Productivity of Siberian Larch Forest Ecosystems. In *Permafrost Ecosystems: Siberian Larch Forests*; Osawa, A., Zyryanova, O.A., Matsuura, Y., Kajimoto, T., Wein, R.W., Eds.; Ecological Studies; Springer: Dordrecht, The Netherlands, 2010; pp. 99–122. ISBN 978-1-4020-9693-8.
21. Osawa, A.; Matsuura, Y.; Kajimoto, T. Characteristics of Permafrost Forests in Siberia and Potential Responses to Warming Climate. In *Permafrost Ecosystems: Siberian Larch Forests*; Osawa, A., Zyryanova, O.A., Matsuura, Y., Kajimoto, T., Wein, R.W., Eds.; Ecological Studies; Springer: Dordrecht, The Netherlands, 2010; pp. 459–481. ISBN 978-1-4020-9693-8.
22. Sofronov, M.A.; Volokitina, A.V. Wildfire Ecology in Continuous Permafrost Zone. In *Permafrost Ecosystems: Siberian Larch Forests*; Osawa, A., Zyryanova, O.A., Matsuura, Y., Kajimoto, T., Wein, R.W., Eds.; Ecological Studies; Springer: Dordrecht, The Netherlands, 2010; pp. 59–82. ISBN 978-1-4020-9693-8.
23. Serreze, M.C.; Walsh, J.E.; Chapin, F.S.; Osterkamp, T.; Dyurgerov, M.; Romanovsky, V.; Oechel, W.C.; Morison, J.; Zhang, T.; Barry, R.G. Observational Evidence of Recent Change in the Northern High-Latitude Environment. *Clim. Chang.* **2000**, *46*, 159–207. [CrossRef]
24. Reichstein, M.; Bahn, M.; Ciais, P.; Frank, D.; Mahecha, M.D.; Seneviratne, S.I.; Zscheischler, J.; Beer, C.; Buchmann, N.; Frank, D.C.; et al. Climate Extremes and the Carbon Cycle. *Nature* **2013**, *500*, 287–295. [CrossRef] [PubMed]
25. Seidl, R.; Thom, D.; Kautz, M.; Martin-Benito, D.; Peltoniemi, M.; Vacchiano, G.; Wild, J.; Ascoli, D.; Petr, M.; Honkaniemi, J.; et al. Forest Disturbances under Climate Change. *Nat. Clim. Chang.* **2017**, *7*, 395–402. [CrossRef]
26. McDowell, N.G.; Michaletz, S.T.; Bennett, K.E.; Solander, K.C.; Xu, C.; Maxwell, R.M.; Middleton, R.S. Predicting Chronic Climate-Driven Disturbances and Their Mitigation. *Trends Ecol. Evol.* **2018**, *33*, 15–27. [CrossRef] [PubMed]
27. Cross, W.F.; Hood, J.M.; Benstead, J.P.; Huryn, A.D.; Nelson, D. Interactions between Temperature and Nutrients across Levels of Ecological Organization. *Glob. Chang. Biol.* **2015**, *21*, 1025–1040. [CrossRef] [PubMed]
28. Zhu, J.; Hu, H.; Tao, S.; Chi, X.; Li, P.; Jiang, L.; Ji, C.; Zhu, J.; Tang, Z.; Pan, Y.; et al. Carbon Stocks and Changes of Dead Organic Matter in China's Forests. *Nat. Commun.* **2017**, *8*, 151. [CrossRef]
29. Alster, C.J.; von Fischer, J.C.; Allison, S.D.; Treseder, K.K. Embracing a New Paradigm for Temperature Sensitivity of Soil Microbes. *Glob. Chang. Biol.* **2020**, *26*, 3221–3229. [CrossRef]
30. Sierra, C.A. Temperature Sensitivity of Organic Matter Decomposition in the Arrhenius Equation: Some Theoretical Considerations. *Biogeochemistry* **2012**, *108*, 1–15. [CrossRef]
31. Mukhin, V.; Voronin, P. Methane Emission during Wood Fungal Decomposition. *Dokl. Biol. Sci.* **2007**, *413*, 159–160. [CrossRef]

32. Abril, G.; Parize, M.; Pérez, M.A.P.; Filizola, N. Wood Decomposition in Amazonian Hydropower Reservoirs: An Additional Source of Greenhouse Gases. *J. S. Am. Earth Sci.* **2013**, *44*, 104–107. [CrossRef]
33. Covey, K.R.; Wood, S.A.; Warren, R.J.; Lee, X.; Bradford, M.A. Elevated Methane Concentrations in Trees of an Upland Forest. *Geophys. Res. Lett.* **2012**, *39*. [CrossRef]
34. Warner, D.L.; Villarreal, S.; McWilliams, K.; Inamdar, S.; Vargas, R. Carbon Dioxide and Methane Fluxes From Tree Stems, Coarse Woody Debris, and Soils in an Upland Temperate Forest. *Ecosystems* **2017**, *20*, 1205–1216. [CrossRef]
35. Carmichael, M.J.; Helton, A.M.; White, J.C.; Smith, W.K. Standing Dead Trees Are a Conduit for the Atmospheric Flux of CH_4 and CO_2 from Wetlands. *Wetlands* **2018**, *38*, 133–143. [CrossRef]
36. Covey, K.R.; Megonigal, J.P. Methane Production and Emissions in Trees and Forests. *New Phytol.* **2019**, *222*, 35–51. [CrossRef]
37. Lyu, Z.; Shao, N.; Akinyemi, T.; Whitman, W.B. Methanogenesis. *Curr. Biol.* **2018**, *28*, R727–R732. [CrossRef]
38. Keppler, F.; Boros, M.; Frankenberg, C.; Lelieveld, J.; McLeod, A.; Pirttilä, A.M.; Röckmann, T.; Schnitzler, J.-P.; Keppler, F.; Boros, M.; et al. Methane Formation in Aerobic Environments. *Environ. Chem.* **2009**, *6*, 459–465. [CrossRef]
39. Lenhart, K.; Bunge, M.; Ratering, S.; Neu, T.R.; Schüttmann, I.; Greule, M.; Kammann, C.; Schnell, S.; Müller, C.; Zorn, H.; et al. Evidence for Methane Production by Saprotrophic Fungi. *Nat. Commun.* **2012**, *3*, 1046. [CrossRef]
40. Stein, L.Y. Methane Oxidation. In *Encyclopedia of Astrobiology*; Gargaud, M., Irvine, W.M., Amils, R., Cleaves, H.J., Pinti, D., Cernicharo Quintanilla, J., Viso, M., Eds.; Springer: Berlin/Heidelberg, Germany, 2019; pp. 1–4. ISBN 978-3-642-27833-4.
41. Quay, P.; Stutsman, J.; Wilbur, D.; Snover, A.; Dlugokencky, E.; Brown, T. The Isotopic Composition of Atmospheric Methane. *Glob. Biogeochem. Cycles* **1999**, *13*, 445–461. [CrossRef]
42. Keppler, F.; Hamilton, J.T.G.; Braß, M.; Röckmann, T. Methane Emissions from Terrestrial Plants under Aerobic Conditions. *Nature* **2006**, *439*, 187–191. [CrossRef] [PubMed]
43. Craig, H. The Geochemistry of the Stable Carbon Isotopes. *Geochim. Cosmochim. Acta* **1953**, *3*, 53–92. [CrossRef]
44. Coplen, T.B. Discontinuance of SMOW and PDB. *Nature* **1995**, *375*, 285. [CrossRef]
45. Wagner, T.; Magill, C.R.; Herrle, J.O. Carbon Isotopes. In *Encyclopedia of Geochemistry: A Comprehensive Reference Source on the Chemistry of the Earth*; White, W.M., Ed.; Springer International Publishing: Cham, Switzerland, 2018; pp. 194–204. ISBN 978-3-319-39312-4.
46. Bréas, O.; Guillou, C.; Reniero, F.; Wada, E. The Global Methane Cycle: Isotopes and Mixing Ratios, Sources and Sinks. *Isot. Environ. Health Stud.* **2001**, *37*, 257–379. [CrossRef] [PubMed]
47. Whiticar, M.J. Carbon and Hydrogen Isotope Systematics of Bacterial Formation and Oxidation of Methane. *Chem. Geol.* **1999**, *161*, 291–314. [CrossRef]
48. Henn, M.R.; Chapela, I.H. Differential C Isotope Discrimination by Fungi during Decomposition of C3- and C4-Derived Sucrose. *Appl. Environ. Microbiol.* **2000**, *66*, 4180–4186. [CrossRef] [PubMed]
49. Fernandez, I.; Mahieu, N.; Cadisch, G. Carbon Isotopic Fractionation during Decomposition of Plant Materials of Different Quality. *Glob. Biogeochem. Cycles* **2003**, *17*. [CrossRef]
50. Fernandez, I.; Cadisch, G. Discrimination against 13C during Degradation of Simple and Complex Substrates by Two White Rot Fungi. *Rapid Commun. Mass Spectrom.* **2003**, *17*, 2614–2620. [CrossRef]
51. Barker, J.F.; Fritz, P. Carbon Isotope Fractionation during Microbial Methane Oxidation. *Nature* **1981**, *293*, 289–291. [CrossRef]
52. Coleman, D.D.; Risatti, J.B.; Schoell, M. Fractionation of Carbon and Hydrogen Isotopes by Methane-Oxidizing Bacteria. *Geochim. Cosmochim. Acta* **1981**, *45*, 1033–1037. [CrossRef]
53. Holler, T.; Wegener, G.; Knittel, K.; Boetius, A.; Brunner, B.; Kuypers, M.; Widdel, F. Substantial 13C/12C and D/H Fractionation during Anaerobic Oxidation of Methane by Marine Consortia Enriched in Vitro. *Environ. Microbiol. Rep.* **2009**, *1*, 370–376. [CrossRef]
54. Uhlig, C.; Loose, B. Using Stable Isotopes and Gas Concentrations for Independent Constraints on Microbial Methane Oxidation at Arctic Ocean Temperatures. *Limnol. Oceanogr. Methods* **2017**, *15*, 737–751. [CrossRef]
55. Wang, C.; Bond-Lamberty, B.; Gower, S.T. Environmental Controls on Carbon Dioxide Flux from Black Spruce Coarse Woody Debris. *Oecologia* **2002**, *132*, 374–381. [CrossRef]
56. Olajuyigbe, S.; Tobin, B.; Nieuwenhuis, M. Temperature and Moisture Effects on Respiration Rate of Decomposing Logs in a Sitka Spruce Plantation in Ireland. *For. Int. J. For. Res.* **2012**, *85*, 485–496. [CrossRef]
57. Yoon, T.K.; Noh, N.J.; Kim, S.; Han, S.; Son, Y. Coarse Woody Debris Respiration of Japanese Red Pine Forests in Korea: Controlling Factors and Contribution to the Ecosystem Carbon Cycle. *Ecol. Res.* **2015**, *30*, 723–734. [CrossRef]
58. Yoon, T.K.; Han, S.; Lee, D.; Han, S.H.; Noh, N.J.; Son, Y. Effects of Sample Size and Temperature on Coarse Woody Debris Respiration from Quercus Variabilis Logs. *J. For. Res.* **2014**, *19*, 249–259. [CrossRef]
59. Chambers, J.Q.; Schimel, J.P.; Nobre, A.D. Respiration from Coarse Wood Litter in Central Amazon Forests. *Biogeochemistry* **2001**, *52*, 115–131. [CrossRef]
60. Wu, J.; Zhang, X.; Wang, H.; Sun, J.; Guan, D. Respiration of Downed Logs in an Old-Growth Temperate Forest in North-Eastern China. *Scand. J. For. Res.* **2010**, *25*, 500–506. [CrossRef]
61. Liu, W.H.; Bryant, D.M.; Hutyra, L.R.; Saleska, S.R.; Hammond-Pyle, E.; Curran, D.; Wofsy, S.C. Woody Debris Contribution to the Carbon Budget of Selectively Logged and Maturing Mid-Latitude Forests. *Oecologia* **2006**, *148*, 108. [CrossRef] [PubMed]
62. Middle Siberia. Natural Conditions and Natural Resources of USSR. Available online: https://litmy.ru/knigi/estesstv_nauki/342782-srednyaya-sibir-prirodnye-usloviya-i-estestvennye-resursy-sssr.html (accessed on 23 December 2020).

63. Peel, M.C.; Finlayson, B.L.; McMahon, T.A. Updated World Map of the Köppen-Geiger Climate Classification. *Hydrol. Earth Syst. Sci.* **2007**, *11*, 1633–1644. [CrossRef]
64. Fraver, S.; Wagner, R.G.; Day, M. Dynamics of Coarse Woody Debris Following Gap Harvesting in the Acadian Forest of Central Maine, USA. *Can. J. For. Res.* **2011**. [CrossRef]
65. Olesen, P.O. Water Displacement Method; a Fast and Accurate Method of Determining the Green Volume of Wood Samples. *For. Tree Improv.* **1971**, *3*, 3–23.
66. Craig, H. Isotopic Standards for Carbon and Oxygen and Correction Factors for Mass-Spectrometric Analysis of Carbon Dioxide. *Geochim. Cosmochim. Acta* **1957**, *12*, 133–149. [CrossRef]
67. Grossman, E.L.; Cifuentes, L.A.; Cozzarelli, I.M. Anaerobic Methane Oxidation in a Landfill-Leachate Plume. *Environ. Sci. Technol.* **2002**, *36*, 2436–2442. [CrossRef] [PubMed]
68. Berg, B.; McClaugherty, C. *Plant Litter: Decomposition, Humus Formation, Carbon Sequestration*, 2nd ed.; Springer: Berlin, Germany, 2008; ISBN 978-3-540-74922-6.
69. Holub, S.M.; Spears, J.D.; Lajtha, K. A Reanalysis of Nutrient Dynamics in Coniferous Coarse Woody Debris. *Can. J. For. Res.* **2001**, *31*, 1894–1902. [CrossRef]
70. Laiho, R.; Prescott, C.E. Decay and Nutrient Dynamics of Coarse Woody Debris in Northern Coniferous Forests: A Synthesis. *Can. J. For. Res.* **2004**, *34*, 763–777. [CrossRef]
71. Palviainen, M.; Finér, L.; Laiho, R.; Shorohova, E.; Kapitsa, E.; Vanha-Majamaa, I. Carbon and Nitrogen Release from Decomposing Scots Pine, Norway Spruce and Silver Birch Stumps. *For. Ecol. Manag.* **2010**, *259*, 390–398. [CrossRef]
72. Köster, K.; Metslaid, M.; Engelhart, J.; Köster, E. Dead Wood Basic Density, and the Concentration of Carbon and Nitrogen for Main Tree Species in Managed Hemiboreal Forests. *For. Ecol. Manag.* **2015**, *354*, 35–42. [CrossRef]
73. Mukhortova, L.V. Carbon and Nutrient Release during Decomposition of Coarse Woody Debris in Forest Ecosystems of Central Siberia. *Folia For. Ser. For.* **2012**, *54*, 71–83. [CrossRef]
74. Rajala, T.; Peltoniemi, M.; Pennanen, T.; Mäkipää, R. Fungal Community Dynamics in Relation to Substrate Quality of Decaying Norway Spruce (*Picea Abies* [L.] Karst.) Logs in Boreal Forests. *FEMS Microbiol. Ecol.* **2012**, *81*, 494–505. [CrossRef] [PubMed]
75. Bebber, D.P.; Watkinson, S.C.; Boddy, L.; Darrah, P.R. Simulated Nitrogen Deposition Affects Wood Decomposition by Cord-Forming Fungi. *Oecologia* **2011**, *167*, 1177–1184. [CrossRef]
76. Mukhortova, L.V.; Kirdyanov, A.V.; Myglan, V.S.; Guggenberger, G. Wood Transformation in Dead-Standing Trees in the Forest-Tundra of Central Siberia. *Biol. Bull. Russ. Acad. Sci.* **2009**, *36*, 58–65. [CrossRef]
77. Yatskov, M.; Harmon, M.E.; Krankina, O.N. A Chronosequence of Wood Decomposition in the Boreal Forests of Russia. *Can. J. For. Res.* **2003**, *33*, 1211–1226. [CrossRef]
78. Rasigraf, O.; Vogt, C.; Richnow, H.-H.; Jetten, M.S.M.; Ettwig, K.F. Carbon and Hydrogen Isotope Fractionation during Nitrite-Dependent Anaerobic Methane Oxidation by Methylomirabilis Oxyfera. *Geochim. Cosmochim. Acta* **2012**, *89*, 256–264. [CrossRef]
79. Kinnaman, F.S.; Valentine, D.L.; Tyler, S.C. Carbon and Hydrogen Isotope Fractionation Associated with the Aerobic Microbial Oxidation of Methane, Ethane, Propane and Butane. *Geochim. Cosmochim. Acta* **2007**, *71*, 271–283. [CrossRef]
80. Rajala, T.; Tuomivirta, T.; Pennanen, T.; Mäkipää, R. Habitat Models of Wood-Inhabiting Fungi along a Decay Gradient of Norway Spruce Logs. *Fungal Ecol.* **2015**, *18*, 48–55. [CrossRef]
81. Mäkipää, R.; Leppänen, S.M.; Sanz Munoz, S.; Smolander, A.; Tiirola, M.; Tuomivirta, T.; Fritze, H. Methanotrophs Are Core Members of the Diazotroph Community in Decaying Norway Spruce Logs. *Soil Biol. Biochem.* **2018**, *120*, 230–232. [CrossRef]
82. Rajala, T.R.; Peltoniemi, M.P.; Pennanen, T.P.; Mäkipää, R.M. Relationship between Wood-Inhabiting Fungi Determined by Molecular Analysis (Denaturing Gradient Gel Electrophoresis) and Quality of Decaying Logs. *Can. J. For. Res.* **2010**. [CrossRef]
83. Herrmann, S.; Bauhus, J. Effects of Moisture, Temperature and Decomposition Stage on Respirational Carbon Loss from Coarse Woody Debris (CWD) of Important European Tree Species. *Scand. J. For. Res.* **2013**, *28*, 346–357. [CrossRef]
84. Bond-Lamberty, B.; Wang, C.; Gower, S.T. Annual Carbon Flux from Woody Debris for a Boreal Black Spruce Fire Chronosequence. *J. Geophys. Res. Atmos.* **2002**, *107*, WFX 1-1–WFX 1-10. [CrossRef]
85. Köster, E.; Köster, K.; Berninger, F.; Prokushkin, A.; Aaltonen, H.; Zhou, X.; Pumpanen, J. Changes in Fluxes of Carbon Dioxide and Methane Caused by Fire in Siberian Boreal Forest with Continuous Permafrost. *J. Environ. Manag.* **2018**, *228*, 405–415. [CrossRef] [PubMed]
86. Masyagina, O.V.; Evgrafova, S.Y.; Menyailo, O.V.; Mori, S.; Koike, T.; Prokushkin, S.G. Age-Dependent Changes in Soil Respiration and Associated Parameters in Siberian Permafrost Larch Stands Affected by Wildfire. *Forests* **2021**, *12*, 107. [CrossRef]
87. Grodnitskaya, I.D.; Sorokin, N.D.; Evgrafova, S.Y.; Antonov, G.I.; Syrtsov, S.N.; Aleksandrov, D.E.; Trusova, M.Y.; Koroban, N.V. Microbial transformation of carbon CH_4 and CO_2 in permafrost-affected soils in tundra and forest ecosystems in Siberia. *Lesovedenie* **2017**, *2*, 111–127.
88. Wall, D.H.; Bradford, M.A.; John, M.G.S.; Trofymow, J.A.; Behan-Pelletier, V.; Bignell, D.E.; Dangerfield, J.M.; Parton, W.J.; Rusek, J.; Voigt, W.; et al. Global Decomposition Experiment Shows Soil Animal Impacts on Decomposition Are Climate-Dependent. *Glob. Chang. Biol.* **2008**, *14*, 2661–2677. [CrossRef]
89. Adair, E.C.; Parton, W.J.; Grosso, S.J.D.; Silver, W.L.; Harmon, M.E.; Hall, S.A.; Burke, I.C.; Hart, S.C. Simple Three-Pool Model Accurately Describes Patterns of Long-Term Litter Decomposition in Diverse Climates. *Glob. Chang. Biol.* **2008**, *14*, 2636–2660. [CrossRef]

90. Boddy, L. Effect of Temperature and Water Potential on Growth Rate of Wood-Rotting Basidiomycetes. *Trans. Br. Mycol. Soc.* **1983**, *80*, 141–149. [CrossRef]
91. Rayner, A.D.M.; Boddy, L. Fungal Decomposition of Wood. Its Biology and Ecology. In *Fungal Decomposition of Wood. Its Biology and Ecology*; John Wiley & Sons Ltd.: Hoboken, NJ, USA, 1988.
92. Griffith, G.S.; Boddy, L. Fungal Decomposition of Attached Angiosperm Twigs. *New Phytol.* **1991**, *117*, 259–269. [CrossRef]
93. Criquet, S.; Ferre, E.; Farnet, A.M.; Le petit, J. Annual Dynamics of Phosphatase Activities in an Evergreen Oak Litter: Influence of Biotic and Abiotic Factors. *Soil Biol. Biochem.* **2004**, *36*, 1111–1118. [CrossRef]
94. Baldrian, P.; Šnajdr, J.; Merhautová, V.; Dobiášová, P.; Cajthaml, T.; Valášková, V. Responses of the Extracellular Enzyme Activities in Hardwood Forest to Soil Temperature and Seasonality and the Potential Effects of Climate Change. *Soil Biol. Biochem.* **2013**, *56*, 60–68. [CrossRef]
95. A'Bear, A.D.; Jones, T.H.; Kandeler, E.; Boddy, L. Interactive Effects of Temperature and Soil Moisture on Fungal-Mediated Wood Decomposition and Extracellular Enzyme Activity. *Soil Biol. Biochem.* **2014**, *70*, 151–158. [CrossRef]
96. Käärik, A.A. 5-Decomposition of Wood. In *Biology of Plant Litter Decomposition*; Dickinson, C.H., Pugh, G.J.F., Eds.; Academic Press: New York, NY, USA, 1974; pp. 129–174. ISBN 978-0-12-215001-2.
97. Schmidt, O.; Czeschlik, D. *Wood and Tree Fungi: Biology, Damage, Protection, and Use*; Springer: Berlin, Germany, 2006; ISBN 978-3-540-32138-5.
98. Harmon, M.E. Ecology of Coarse Woody Debris in Temperate Ecosystems. *Adv. Ecol. Res.* **1986**, *15*, 133–302.
99. Rinne-Garmston, K.T.; Peltoniemi, K.; Chen, J.; Peltoniemi, M.; Fritze, H.; Mäkipää, R. Carbon Flux from Decomposing Wood and Its Dependency on Temperature, Wood N2 Fixation Rate, Moisture and Fungal Composition in a Norway Spruce Forest. *Glob. Chang. Biol.* **2019**, *25*, 1852–1867. [CrossRef] [PubMed]
100. Jomura, M.; Kominami, Y.; Dannoura, M.; Kanazawa, Y. Spatial Variation in Respiration from Coarse Woody Debris in a Temperate Secondary Broad-Leaved Forest in Japan. *For. Ecol. Manag.* **2008**, *255*, 149–155. [CrossRef]
101. Forrester, J.A.; Mladenoff, D.J.; Gower, S.T.; Stoffel, J.L. Interactions of Temperature and Moisture with Respiration from Coarse Woody Debris in Experimental Forest Canopy Gaps. *For. Ecol. Manag.* **2012**, *265*, 124–132. [CrossRef]
102. Pettersen, R.C. The Chemical Composition of Wood. In *The Chemistry of Solid Wood*; Advances in Chemistry; American Chemical Society: Washington, DC, USA, 1984; Volume 207, pp. 57–126. ISBN 978-0-8412-0796-7.
103. Gough, C.M.; Vogel, C.S.; Kazanski, C.; Nagel, L.; Flower, C.E.; Curtis, P.S. Coarse Woody Debris and the Carbon Balance of a North Temperate Forest. *For. Ecol. Manag.* **2007**, *244*, 60–67. [CrossRef]
104. Ivanov, A.V.; Braun, M.; Zamolodchikov, D.G.; Loshakov, S.Y.; Pototskii, O.V. Carbon Emission from the Surface of Coarse Woody Debris in Korean Pine Forests of Southern Primorye. *Russ. J. Ecol.* **2018**, *49*, 306–311. [CrossRef]
105. Mackensen, J.; Bauhus, J.; Webber, E. Decomposition Rates of Coarse Woody Debris—A Review with Particular Emphasis on Australian Tree Species. *Aust. J. Bot.* **2003**, *51*, 27–37. [CrossRef]
106. Carrier, M.; Auret, L.; Bridgwater, A.; Knoetze, J.H. Using Apparent Activation Energy as a Reactivity Criterion for Biomass Pyrolysis. *Energy Fuels* **2016**, *30*, 7834–7841. [CrossRef]